Chapter 7
Biomedical Applications

Ignazio Roppolo, Annalisa Chiappone, Alessandro Chiadò, Gianluca Palmara, and Francesca Frascella

Abstract In recent years, 3D printing technology has become a sufficiently mature technique to allow not only the production of objects starting from a design modeling but also a possible customization through the introduction of functionality by the end user. This rapid prototyping technique represents a very promising technology for device fabrication with different application fields (e.g., biological, environmental, food, aerospace), offering advantages over traditional manufacturing methods.

Moreover, the 3D printing archetype has introduced novel opportunities for the realization of smart devices, where the added value lies in their intrinsic functionality. In fact, 3D-printed functional materials can transform their structure in response to specific stimuli (e.g., temperature, pH, light radiation, etc.), adding to the printed object interesting properties to take advantage of. Recently, this paradigm has been explored and expanded by researcher's/engineer's community with the aim of realizing 3D printable objects that present exploitable chemical functionalities.

In this chapter, functional 3D objects for bio-applications have been reported, combining 3D printing technology with an accurate material engineering. The result is a single step 3D-printed object with intrinsic chemical functionalities that could be exploited to produce immunoassay-based and/or enzymatically active devices for biosensing purposes and precision medicine.

Keywords 3D printing · Functionality · Biosensors · Biorecognition · Biocatalysis · Precision medicine

I. Roppolo · A. Chiadò · G. Palmara · F. Frascella (✉)
Department of Applied Science and Technology – DISAT, Politecnico di Torino, Torino, Italy
e-mail: francesca.frascella@polito.it

A. Chiappone
Department of Chemical and Geological Sciences, Università di Cagliari, Cittadella delle Scienze, Monserrato, Italy

S. L. Marasso, M. Cocuzza (eds.), *High Resolution Manufacturing from 2D to 3D/4D Printing*, https://doi.org/10.1007/978-3-031-13779-2_7

7.1 Introduction

The rapid evolution of 3D printing technology in the last 20 years demonstrated that this technique has the potential to revolutionize the manufacturing processes in many industrial fields such as automotive, aerospace and aviation, medicine, and healthcare, as well as to be disruptive in academia [1]. 3D printing, or alternatively mentioned as additive manufacturing (AM), is an umbrella term that comprehends a wide set of technologies, which has in common the ability to produce 3D objects starting from digital objects designed by computer-aided design (CAD) software or 3D scanners. These models are then generally transformed in STL files (which acronym stays for standard tessellation language or standard triangle language), which are used by the 3D printer, after a slicing of the file in cross-sections, to define the controlled deposition of material layer by layer, until the complete fabrication of the object. One of the main advantages of 3D printing consists of the fast and relatively cheap fabrication of prototypes, avoiding tooling and time-consuming post processing. Furthermore, compared to conventional subtractive manufacturing processes, it allows higher personalization and the fabrication of more complex geometries [2]. Nowadays, 3D printing is mainly employed in manufacturing of small series where the primary goal is to obtain nearly finished products, because it allows faster modification and optimization of parts compared to high-volume production [3]. For example, nanocomposite polymeric materials are often employed in 3D printing to improve the mechanical properties of the final object [4]. Moreover, the use of engineered materials in 3D printing is exploited to fabricate objects with additional properties, enhancing their functionalities adding another grade of complexity to the structural or chemical properties. Those functional materials are typically studied to provide new intrinsic properties to the components, either with or without external stimuli; from this aroused the concept of 4D printing, as further development of 3D printing [5, 6]. Under the umbrella term "4D printed" are considered all the 3D-printed objects that can undergo shape-shifting in response to an external stimulus, for example, pressure, temperature, magnetic fields, or light [5–7]. Similarly, some authors proposed to use the same paradigm to objects that possess intrinsic biochemical functionalities [6]. In this frame, active devices for biotechnological applications have been reported, exploiting functional 3D objects with biorecognition and/or catalytic capabilities.

In this chapter, different types of devices fabricated by 3D printing technology exploited to perform bioanalytical analysis will be presented, focusing on the materials' design to achieve those smart objects exploiting intrinsic and/or tunable functionalities. In fact, 3D printing field showed increasing attention to bio-applications, most of all in tissue engineering and regenerative medicine [8, 9] or in the rapid prototyping and fabrication of components for biomedical purposes [10–13]. Recently, the field of fabrication of 3D-printed constructs for tissue engineering and regenerative medicine has been comprehensively reviewed [14–17]. Instead, this chapter aims to evidence the relationship between material design and the presence of (bio)chemical functionalities in 3D-printed devices, which will be

listed in different bio-applications such as biorecognition, biocatalysis, flexible and wearable sensors, and precision medicine. Before, to deepen those aspects, the working principles of the most common 3D printing methods will be presented, describing advantages and limitations. At last, future perspectives of the most novel trends in this advanced field will be discussed.

7.2 Additive Manufacturing (AM) Techniques for Biomedical Applications

On the market, several 3D printing techniques to process polymeric materials are present; nevertheless, those can be classified in three main categories, based on the underlying mechanism: the extrusion-based methods, the powder-based methods, and at last the light-induced methods (i.e., based on photopolymerization) [18–20]. Obviously, every 3D printing process presents its advantages and disadvantages if compared with the others. When a type of printing process is chosen, it must be taken into account the specific application as well as the materials to be used and the resolution requested [21]. Coming back to the specific of the techniques, those are usually defined as follows:

- Extrusion-based methods: AM process in which material is spread by means of a nozzle or a printing head [18].
- Powder-based methods: AM process in which powders are locally softened/melted by a controlled heating [20].
- Photopolymerization (light-induced) methods: AM process in which liquid monomer is rapidly solidified by light irradiation [21].

Each of these categories contains different equipment types, which may differ for construction approaches or material deposition. The most common are summarized in Table 7.1.

In the following paragraphs, the most diffused 3D printing methods used to fabricate objects with built-in (bio)chemical functionalities for biotechnological applications will be briefly introduced.

7.2.1 Additive Manufacturing: Extrusion-Based Methods

7.2.1.1 Fused Filament Fabrication

Fused filament fabrication (FFF) is the most diffused and acknowledged 3D printing method, also commonly known with the name FDM™ (fused deposition modeling), trademarked from Stratasys. At the present, FFF 3D printers are largely present in day-by-day experience, from big industries to houses for DIY modeling. Those 3D printers are employed in a wide range of applications, thanks to the large platelet of

Table 7.1 Categories of additive manufacturing processes, materials, and advantages vs. limitations

Additive manufacturing	Main techniques	Materials	Pro	Cons
Extrusion	Fused filament formation (FFF)	Thermoplastics	Multi-material, versatile, and low cost	Limited resolution Post processing
	Direct ink writing (DIW)	Plastics, food, and living cells	Versatile	Limited resolution
	Bioprinters	Chemical and physical gels and living cells	Specifically designed for bio-applications	Limited resolution
Powder bed	Selective laser sintering (SLS)	Thermoplastics	High mechanical properties No need of supports	Low resolution Limited range of printable materials
Photopolymerization	Stereolithography (SLA) Digital light processing (DLP), Continuous liquid interface polymerization (CLIP) Volume additive manufacturing (VAM)	Photopolymers	High range of printable materials High resolution	Single material
	Two-photon polymerization (TPP)	Photopolymers	Extremely high resolution	Low yield of production Expensive
	Photopolymer jetting (inkjet/Polyjet)	Photopolymers	Simple, multi-material	Limited range of printable materials

commercially available materials, to the large range of printing dimensions, and to their user-friendly and affordability [22]. Nowadays, when one thinks to 3D printing, FFF is the first technique to which the most refers to [23].

Feeding materials for an FFF 3D printer are wires or filaments, which are softened/melted and extruded through a heated nozzle, depositing the material on the build platform accordingly to the STL file. The softened filament solidifies cooling down, allowing the fabrication of the object in a layer-by-layer fashion [18].

Only thermoplastic polymeric materials (i.e., not cross-linked macromolecules) can be available for FFF because they must be softened; both amorphous (e.g., polystyrene, polycarbonate, ABS – acrylonitrile butadiene styrene) and crystalline (e.g., PLA, polylactic acid; PEEK, polyetheretherketone; nylon) materials can be processed [24].

The printing resolution belongs to the dimension of the extruding head, as well as by rheological issues (viscosity, temperature, speed of printing, etc.). Considering the 3D printers now available on the market, the highest declared resolution is about 10 μm, but for most of the equipment, it is about 50 μm. On the other hand, even layer thickness (i.e., slicing of the virtual file) is directly related to the dimension of the extruded filament, so the build rate decreases increasing the resolution, involving a suitable trade-off must [25].

One of the limits of FFF is in the extent of available geometries that could be printed, in particular regarding the hanging parts or large voids. In this case, the fabrication is necessary to use supports, often using a second material, which must be removed afterward with mechanical or chemical approaches.

Regarding the characteristics of the printed objects, interlayer adhesion, which belongs on many factors including the temperature of extrusion, the heat transfer of the material, the temperature of the build platform, and the geometry of the object, can be an issue. Poor adhesion weakens the object, leading to low mechanical properties and possible delamination. At last, the presence of porosity and defects decreases the mechanical performances and ultimately brings to failure [23].

Besides, FFF presents several advantages when compared to other 3D printing techniques. The most exploited one is to print multiple material in the same part (multi-material printing). This is achieved by using multiple nozzles, each one with a different filament: this enables a topological control of the chemical and physical properties of the part [26, 27]. Furthermore, FFF is the most common choice for rapid prototyping and hobby because of the low costs, the ease of use, and the absence of hazardous raw materials. At the present stage, there is an almost infinite range of FFF 3D printers available on the market, which cover a broad range of materials, printing dimensions, and of course prices (from few hundreds of € to hundreds of thousands of € for a single equipment) [28].

7.2.1.2 Direct Ink Writing

Another extrusion-based 3D printing technique is direct ink writing (DIW). Different from FFF, DIW 3D printer extrudes pastes or, in general, viscous liquids,

so materials are already in a liquid form. The viscous inks can be different but typically are constituted of solutions made of polymers in desired solvents (which can be either water or organic solvents), oligomers (i.e., macromolecules with a certain molecular weight) with suitable viscosity, or pastes that contain inorganic fillers bounded with a certain amount of plasticizing macromolecules [29].

A motorized screw and a pressure pump are usually employed to control the extrusion rate, which must be controlled to achieve a uniform extrusion of the paste through the nozzles. Similar to FFF technique, once extruded, the ink is deposited on the build platform, following the relative digital file. In case the extruded material does not have sufficient thixotropic properties to be self-standing and thus to form, layer by layer, the desired object, a rapid change of physical state (i.e., solidification) is used to perform the 3D printing process [30]. Several approaches can be employed; among the most common can be mentioned: rapid solvent evaporation [31], thermal-induced cross-linking [32], chemical-induced cross-linking [33], photo-induced cross-linking [34], and rapid phase transition [35]. There are also other examples since this 3D printing technique is in rapid evolution, for instance, a new DIW approach called "immersion precipitating 3D printing" recently has been introduced. By this method, a polymeric solution is extruded in a non-solvent and rapidly precipitate [36]. This technique allows to produce highly porous polymers, and it demonstrated to be suitable for many polymers in 3D printing.

The main advantages of DIW are its low cost and the compatibility with an extremely wide range of materials, also customizable by the user, together with an extremely flexible approach; also, DIW allows very high resolutions (<10 μm). The main issues in DIW are instead related to the control of the rheological properties of the inks, which is compulsory to obtain homogeneous extrusion and desired precision. Moreover, the rate of solidification must be set according to the printing process, since the fast change of physical state may cause nozzle clogging or bad adhesion between layers, while a slow change can bring to poor mechanical properties and lose of the geometries of the 3D-printed part. At last, operating even with organic solvents, DIW is generally more hazardous than FFF [29].

DIW is used to print different class of materials, not only polymers but also ceramics, colloids, and even wood. In case DIW is applied to soft and biological matter, this technique is known as bioprinting, which will be described more in details in the next paragraph.

7.2.1.3 Bioprinters

Generally speaking, the term "bioprinting" refers to a plethora of laboratory technologies which aims at fabricating biological constructs, primarily to reproduce living tissues [37]. Among the bioprinting equipment, it is worth to mention laser-assisted 3D printers, stereolithography (SLA)-based, pressure-assisted, or droplet-based [38].

This means that bioprinting can be classified in more than one category of the 3D printing techniques (Table 7.1). Nevertheless, the most developed one is the pressure-assisted (extrusion), and the term "bioprinter" is generally used for commercially available equipment able to extrude inks/gels/pastes through a motorized syringe and containing cells. Some of the most diffused commercial brands are EnvisionTEC; Organovo, Inc.; CELLINK; and Rokit Healthcare, Inc.

As all the extrusion-based techniques, bioprinting involves the selective deposition in a layer-by-layer fashion of cyto-compatible materials directly laden with living cells. Extrusion can be pneumatic, piston, or screw-driven, according to the producer. Usually the bioink is a gel, which means that melting or softening is not encompassed in the process even if, according to the equipment employed and to the material specifications, heating or refrigeration can be considered both to the material and on the build plate [39]. Furthermore, even modification of syringes enabled the production of more complex constructs such as embedded printing [40], coaxial printing [41], or in situ cross-linking [42].

Droplet-based bioprinting (DBB) is as well a very common method, even if it could be mostly considered a deposition technique rather than an extrusion-based. In fact, this involves droplet generation and deposition in a continuous or on-demand manner employing a different driving force such as electrical, thermal, or acoustic. Furthermore, DBB allows the printing of proteins or cells encapsulated in droplets, which was also exploited for co-patterning with gel-based scaffold materials. As ink-based technology, DBB is characterized by medium/high resolution (<10 μm in some case) and suitable for high-throughput applications, due to high printing speed. Conversely, the development of real 3D constructs (build on z-axis) is time consuming and not favored [37].

Regarding the printable materials, the primary interest is to print gels able to mimic the extracellular matrix, to aid cells' colonization. Gels can be both natural (e.g., collagen, gelatin, alginate, chitosan) and synthetic (e.g., poly(N-isopropylacrylamide), PEG-based, etc.), or blends of the two [43].

Regarding the applications, as mentioned, the first goal is to embed cells or other biological matter in order to artificially build controlled environments [44]. This can lead to innovative biomedical and pharmaceutical studies, developing artificial organs or tissues, that can be either scaffold-based or scaffold-free, fabricating organ-on-a-chip devices [45], and even reproducing patients' tissues, enabling a new approach to in vivo-like studies [37]. Being specifically developed for bio-matter, bioprinting allows the 3D shape of materials that cannot be processed with other technologies, gathered with the bio-field requirements. The possibility to impart 3D structuration to biomaterial, with controlled morphology, can improve the cell growth remarkably improving the results obtained in conventional bidimensional cell culture [37]. As drawback, the resolution is usually relatively low due to intrinsic material characteristics, and the suitable materials are limited by viscosity and biocompatibility [43].

7.2.2 Additive Manufacturing: Photopolymerization-Based Methods

Photopolymerization-based 3D printing techniques use light as a stimulus enabling the printing mechanism [22]. In fact, all the technologies encompassed in this category use light to produce solid objects through a fast transition from liquid to solid material, by light-induced polymerization mechanism. Many different light curing technologies have been developed and will be described in the following paragraphs [46].

Vat printing techniques are the most diffused light-induced 3D technologies. Again, vat 3D printing includes different methods, but in all of those, the liquid printable photocurable material is placed in a vat during printing procedure; stereolithography (SLA) and digital light processing (DLP) are in this context the two more common technologies. Both are based on the spatially controlled solidification of a liquid resin upon a selective exposure to light, even if performed with different approaches [47]. SLA is historically the first additive manufacturing technology, developed and patented by Charles Hull in the 1980s [48]. In SLA equipment, a laser light source scan point by point the surface of the photocurable resins contained in a vat, inducing controlled photopolymerization and solidification. The process is the repeated layer by layer, moving downward or upward the build platform along the z-axis, according to the printer configuration [22]. DLP is somehow an evolution of SLA. In DLP, the light source (typically a LED centered at 365 nm or 405 nm) illuminates a digital micro-mirror device (DMD), which shine all in one the designed pattern on the bottom of the vat containing the light-sensitive resin. The light source is usually placed below the vat, and in some equipment, the LED/DMD illuminating system is replaced by a LCD screen. In any case, the bottom of the vat must be transparent, and the printing direction is usually bottom-up along the z-axis [22]. A more recent evolution of the DLP technology is the continuous liquid interface polymerization (CLIP) [49] 3D printing, which shortens the printing times exploiting oxygen-induced-free radical polymerization inhibition to avoid the adhesion of the photocured layer to the bottom of the vat. This allows the development of a continuous process in z direction, which is peculiar of this technique. In the latest years, a further light-induced technology named volumetric additive manufacturing (VAM) [50] has been also proposed. Different from the other 3D printing technologies, this technique is not layer by layer but implies the selective light-induced solidification within a contained volume, exploiting the superimposition of patterned optical waves from multiple beams, enabling thus the direct generation of 3D geometries. The best performing light-induced techniques named so far can achieve resolutions at the micrometric scale [22]. Regarding materials in light-based 3D printing, the most common are low molecular weight (meth)acrylate monomers (e.g., polyethylene glycol(meth)acrylate, 1,6-hexanediol diacrylate, bisphenol-A-ethoxylate diacrylate, pentaerythritol tri−/tetra-acrylate). In any case, commercial resins are not detailed mixtures of monomers, formulated to fulfill the desired characteristics together with high printing speed and resolution.

A detailed list of the more commonly used materials can be found in literature [22, 46, 51]. Out of acrylate-based formulations, also thiol-ene/yne and epoxy monomers are employed [24]. To activate the photopolymerization mechanism, the presence of a proper photoinitiator is also necessary, in which range of reactivity should match the wavelength of the 3D printer. Eventually dyes can be also used to improve the printing resolution [22].

On the market, many SLA and DLP equipment are now present, which encompass a large range of dimension and costs, from big industrial 3D printers to cheap desktop ones. While a very important application still remains modeling/hobby and prototyping [52], SLA and DLP equipment are largely used in jewelry [53] and dentistry, due to their high precision and the possibility to create shapes not achievable with other 3D printing technologies [54]. In the academia, they are as well very used, with many reports which span over a broad range of applications such as microfluidics [55], electronics, or sensing [56, 57]. DLP has been used as bioprinting technique, employing an apparatus with light source with low energy coupled with sterilization tools. This demonstrated suitable for the printing of cytocompatible scaffolds embedding living cells [5].

As mentioned, the high resolution that can be achieved is the most important advantage of the light-based techniques, together with the accuracy and the smooth surface obtained. Furthermore, functional molecules or fillers can be easily incorporated in the polymer due to the fact that starting materials are liquid, allowing highly versatility in the development of 3D objects embedding intrinsic functionalities [58]. On the other hand, the main limitation is related to the use of single materials, at least on x-y plane.

7.2.2.1 Two-Photon Polymerization

The 3D printing technology with the highest resolution is two-photon polymerization (TPP), which is based on a nonlinear two-photon absorption process [59]. In TPP, the material reservoir is just a drop of liquid photocurable formulation. Different than other light-induced technologies, here the polymerization mechanism begins when two photons, usually with wavelength in the near-infrared spectrum, are absorbed simultaneously by the photoinitiator, generating the reactive species. This can occur only in a very limited spot (voxel) in which the light source, a femtosecond pulse laser, is focused. This also means that TPP can polymerize the material in any point of the drop, without the need of supports. Out of the focal point, the polymerization does not take place; therefore, the light pass through the material without inducing polymerization. TPP allows to create 3D structures with resolution at the nanometric scale (<100 nm), even if obviously it cannot be used for big object to the prolonged printing times [60]. Also in this case, the materials used are usually (meth)acrylate resins [61].

TPP was proposed for various biological applications such as tissue engineering [62] and medical sensors [63], as well as in other fields such as micromachining or photonics [64, 65]. As mentioned, the main advantage of TPP is the high resolution

that can be reached, while as main drawbacks, there are the very low yield of production and the limitation of the dimensions of the printed objects [61].

7.2.2.2 Photopolymer Jetting

Photopolymer jetting (InkJet/PolyJet) is another light-based technique in which the resin is injected from a printing head to create a two-dimensional pattern. Somehow is like standard inkjet but the drops are thicker and more viscous, enabling a rapid fabrication of a 3D object. After the deposition of every layer, light is provided to solidify the material. Having multiple printing head, it is also easy to fabricate multi-material objects [66].

This technology uses commercial photopolymer resins with precise viscosities. The complex technology required by this equipment leads to nearly complete industrial development, with the most of the marked occupied by Stratasys (PolyJet), which materials are proprietary [67].

With PolyJet, it is possible to produce objects with good resolution with a good variety of commercial materials; nevertheless, the mechanical and functional properties that can be reached are still limited [68, 69].

7.3 3D-Printed Functional Materials for Bio-applications

7.3.1 Biorecognition and Intrinsic Functionality

Biosensors are devices with analytical capabilities that can be used in different applications (i.e., diagnostics, food industry, environmental monitoring) for the specific recognition of different analytes, mostly proteins and small molecules [70]. In this context, 3D printing demonstrated to be effective in the manufacturing biosensing devices, showing several advantages for the fabrication of point-of-care (POC) platforms, devices able to perform testing directly without the support of laboratory equipment [71]. 3D printing has the potentialities to improve the biorecognition and the overall performances (e.g., enhanced sensitivity) when combined with other established recognition techniques, as well as to facilitate the immobilization of the biorecognition elements, as reported in the following.

7.3.1.1 Improved Biorecognition

The synergistic effect of 3D printing together with other techniques may lead to advancements in biotechnological applications, in this case sensing. Gomez and coworkers developed a molecular imprinted polymer (MIP) formulation for TPP [72], selecting N-carbobenzyloxy-L-phenylalanine as model template for the MIP

synthesis. This was done because the fluorescent analogue dansyl-L-phenylalanine is commercially available and allows an easy quantification of the binding properties of the MIP. As a proof of concept, an array of 20 × 60 μm cantilever sensors with embedded MIPs was fabricated (Fig. 7.1a). Incubating the array with the analyte, a reversible shift of the resonant frequency of the sensors was obtained (Fig. 7.1b), enabling the measurement of relative variations of about one order of magnitude more than other commercial micro gravimetric equipment, such as quartz crystal microbalance.

De Middeleer and coworkers used a similar approach to developed 3D-printed solid-phase extraction (SPE) sorbent for mycotoxin analysis [73]. The authors synthesized a MIP using metergoline as a model template for ergot alkaloid recognition and immobilized the artificial receptors on 3D cylindrical poly-ε-caprolactone (PCL) scaffolds, printed by melt extrusion. The functional analysis demonstrated that by employing 3D-printed MIP-based scaffolds, a robust analytical method for multi-mycotoxin testing was developed.

Another system helpful in the recognition of toxins was proposed by Gou et al. In this work, the authors designed a hydrogel matrix embedding functional polydiacetylene nanoparticles, which were exploited both for sensing and detoxification purposes [74]. The functional nanoparticles were synthesized with alkenyl groups on their surface and then chemically immobilized in a 3D poly(ethylene glycol) diacrylate (PEGDA) hydrogel printed using the DLP photopolymerization technique, mimicking a liver structure (Fig. 7.2c, d). After the incubation of this bioinspired device with 50 μg/mL of the toxin dispersed in murine red blood cells, the specific recognition of a pore-forming toxin was demonstrated: thanks to its large specific surface area, the functional 3D hydrogels captured and removed 100% of the toxin, demonstrating thus also a remarkable detoxification efficiency.

Those strategies were not only used to enhance the biorecognition for sensing purposes, but also in separation technology, for instance, chromatography. This technology allows to directly prepare the stationary phase rapidly and without further chemical modifications. In this context, Macdonald et al. reported the fabrication of 3D-printed polymeric thin-layer chromatography (TLC) platforms which were successfully applied for separating various dyes, proteins, and conjugates without any additional surface functionalization [75].

These devices were produced by PolyJet printing employing the commercial resin VeroClear RGD810. With a similar approach, Parker and coworkers reported a 3D-printed microfluidic device incorporating immunoaffinity monoliths for the extraction of preterm birth (PTB) biomarkers [76]. In this case, a glycidyl methacrylate monolith was fabricated in the channel of a 3D-printed device fabricated by stereolithography; the monolith was used as anchoring point for antibodies against the PTB to be detected in human serum matrix. At last, Belka et al. proposed alternative methods for solid-phase extraction of fabricating sorbents with a scabbard-like shape by FFF using LAY-FOMM60, to be used for the analysis of steroids in human plasma [77].

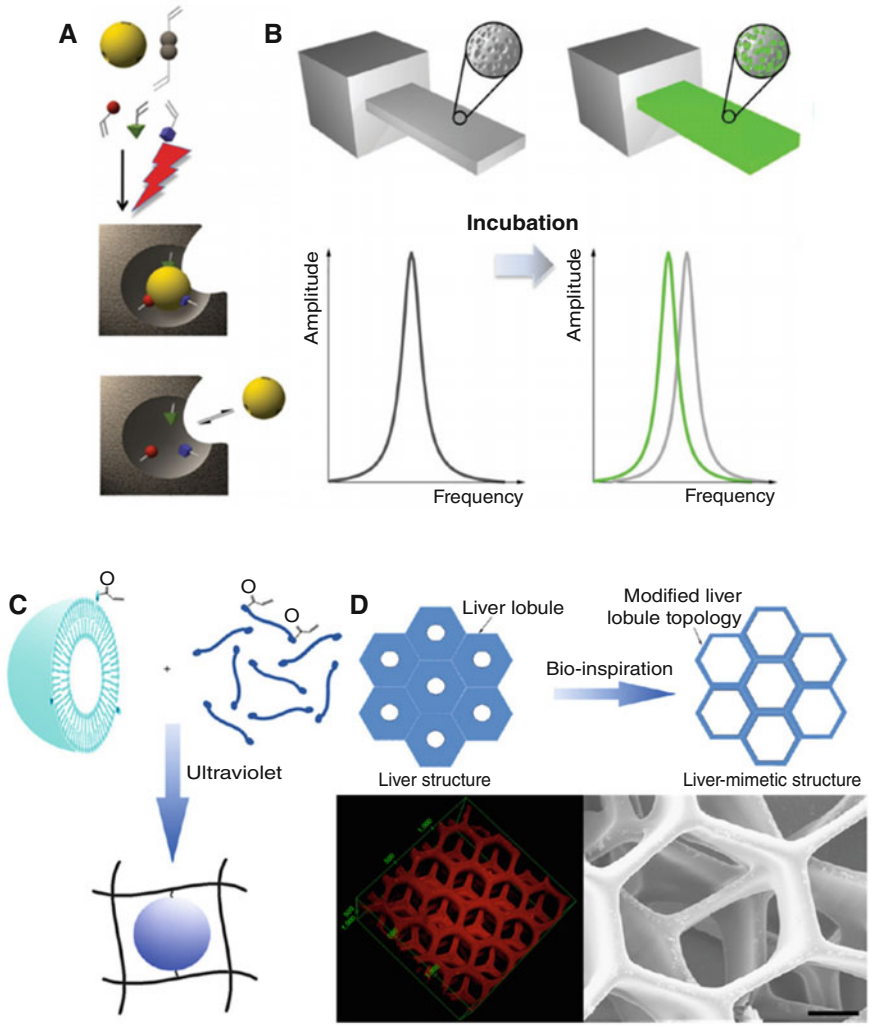

Fig. 7.1 (**a**) Steps of the photo-assisted MIP fabrication. (**b**) MIP cantilever fabricated by TPS and schematics of the sensing principle (Adapted from Ref. [72] with the permission from the Wiley-VCH Verlag). (**c**) Integration of nanoparticles in a photocured PEGDA hydrogel. (**d**) Liver-mimetic microstructure used as detoxifier (top) and its 3D structure measured by laser confocal microscopy and scanning electron microscope (scale bar 50 μm). (Adapted from Ref. [74] with the permission from the Springer Nature)

7.3.1.2 Improved Immobilization

One of the key aspects to successfully obtain a performing sensing layer during the development of biosensors is the controlled and stable immobilization of biorecognition elements [78].

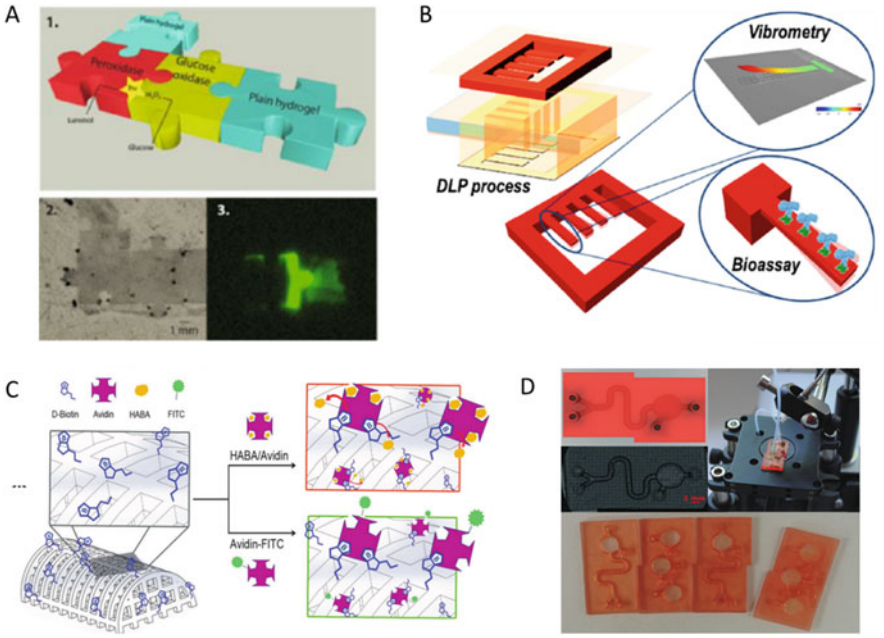

Fig. 7.2 (**a**) Puzzle-shaped 3D-printed PEGDA hydrogels entrapping horseradish peroxidase and glucose oxidase: (1) CAD of the 3D-printed objects and (2) imaging of the printed objects. (3) Chemiluminescent measurements (3 min) in the presence of 100 mM glucose and 220 μM luminol in Veronal buffer 30 mM and KCl 30 mM (Adapted from Ref. [81] Copyright 2016 American Chemical Society). (**b**) Workflow of the fabrication of 3D-printed microcantilever arrays and their vibrational characterization (Adapted from Ref. [82] Copyright 2017 American Chemical Society). (**c**) Schematic of the colorimetric- and fluorescence-based binding assays grafting biotin on 3D-printed microstructures (Reprinted from Ref. [83] with the permission from the WILEY-VCH Verlag). (**d**) CAD, microscope images, and picture of the 3D-printed microfluidic modular LOCs. (Adapted from Ref. [86] with the permission from the Royal Society of Chemistry)

Often, the surface functionalization is the most time-consuming procedure in the fabrication of biosensors [79, 80]; this leads many efforts to the development of 3D-printed objects that could be employed directly or with very limited (bio)chemical modification.

For instance, Mandon and coworkers produced functional 3D-printed objects entrapping biomolecules during the polymerization step [81]. For instance, they chose puzzle shapes as a proof of concept of more complex structures such as a multiplex biosensing layer. The PEGDA-based hydrogel was 3D printed using DLP, fabricating puzzle pieces containing different enzymes (Fig. 7.2a). Once fit together, glucose was used to observe the sequential activity of the two enzymes. Indeed, it was exploited as substrate by the glucose oxidase, producing hydrogen peroxide, which was subsequently used as substrate by the horseradish peroxidase to produce chemiluminescence in the presence of luminol.

Similarly, Stassi et al. fabricated 3D-printed functional microcantilever platform in a one-step process with DLP, which was later used for mass detection [82].

This biosensor was built adding acrylic acid to the bisphenol A ethoxylate diacrylate (BEDA) in a photocurable formulation, introducing a controlled amount of carboxyl groups in the polymeric matrix, which then were exploited as anchoring points for the immobilization of biorecognition elements. The proof of concept was then tested by immunoassays performed on the surface of the microcantilevers (Fig. 7.2b).

Another example of bioactive 3D scaffolds integrated into a monolithic lab-on-chip (LOC) was reported by Credi and coworkers by a stereolithography printing process [83]. In this work, the authors designed a biotin-conjugated UV-curable resin, which was used to produce scaffolds with features smaller than 100 μm and with pore size of 400 μm. HABA (4-hydroxyazobenzene-2-carboxylic acid)/avidin molecules were then employed as a standard biotin binding assay to detect biotin on the surface of the 3D-printed structures. Afterward, the biotinylated scaffolds were integrated in a microfluidic reactor, fluxing the HABA/avidin solution to perform real-time analyses (Fig. 7.2c).

Aronsson and coworkers reported the development of a hybrid peptide-polymer hydrogel, which combines covalent cross-linking with supramolecular interactions, to tune the mechanical properties as well as the biochemical functionalities [84]. The authors used bicyclo[6.1.0]nonyne-modified hyaluronic acid together with an eight-arm PEG bearing terminal azide groups, to take advantage of the click reaction between the alkyne and azide, thus achieving covalent cross-linking. Furthermore, a helix-loop-helix polypeptide able to dimerize into helix bundles was also tethered to the hyaluronic acid backbone: this polypeptide was used to change the cross-linking density and to impart desired mechanical properties to the printed components. At last, biotin conjugation into the polypeptide loop was used to immobilize a streptavidin-AP (alkaline phosphatase), monitoring its activity by using a chromogenic probe.

Intrinsic functionalities embedded in 3D-printed objects were also studied to upgrade well-established techniques, such as enzyme-linked immunosorbent assay (ELISA). This is considered the gold standard for the detection of many analytes, because of its remarkable sensitivity and sensibility [10]. Furthermore, being very versatile (e.g., an antibody can be produced against a wide range of target analytes) and its moderate price, ELISA is often applied in the food analysis to detect traces of contaminants and of pathogens. Conversely, the strict protocol requirements (need for laboratory equipment, protocol optimization related to target analyte, and the use of commercial polystyrene labware) hardly allow to reach the flexibility required to perform analyses outside of clinical or research environments [11].

3D printing technology has been recently investigated to solve these drawbacks, enabling the possibility to implement the ELISA tool in open-field applications. For example, centrifugal microfluidic devices were fabricated using ABS (acrylonitrile butadiene styrene) by PolyJet 3D printing, driven by a mini-centrifuge and employed to perform an ELISA, as reported by Ukita and coworkers [85, 87]. In this study, the colorimetric reaction was evaluated both by means of a

plate reader and a smartphone, showing comparable results. In this framework, Chiadò et al. reported the DLP fabrication of polymeric microfluidic devices, which were then used to detect biomarkers involved in angiogenesis [86]. The authors fabricated modular LOCs with embedded chemical groups which were exploited to immobilize biorecognition elements, thus producing biosensors which implement an immunoassay as detection method. Carboxylic moieties were introduced by adding acrylic acid in three different photocurable monomers that were compared in terms of physicochemical properties and protein grafting capabilities. A formulation with BEDA and 10% wt of acrylic acid was proved to be the best-performing material among all the tested ones, and it was used for the fabrication of a sensing platform composed of a microfluidic channel and an incubation well. The functional polymer was printed only in desired areas, to confine the active material to specific points, increasing the sensitivity and reducing the nonspecific binding on other parts of the LOC (Fig. 7.2d). A sandwich immunoassay and a portable fiber optic spectrometer were used to evaluate the optical density for the detection of vascular endothelial growth factor and angiopoietin-2.

Another kind of sought-after improvement in ELISA-based bioassays is to increase its sensitivity. This was achieved by increasing the available surface area, as demonstrated by Singh and coworkers. They introduced a so-called 3D well, a hollow cylinder-like structure made of ABS fabricated by FFF 3D printing, to study the serological diagnosis of infectious diseases [87, 88]. After the printing process, the surface modification was conducted by chemical etching to show hydrophilic properties, achieving effective protein binding capability, which resulted in higher sensitivity than standard 96-well ELISA toward rubella virus and measles virus (2.25- and 3-folds, respectively).

7.3.1.3 Improved Functionality

The use of composite and nanocomposite materials has always been one common strategy to improve the objects' properties. This can also be applied to the 3D printing field [21] where the addition of fillers into the printable matrices has led to the production of three-dimensional objects with enhanced electrical [89], mechanical [90], or functional [7, 91, 92] properties.

The use of conductive fillers in polymeric matrices (e.g., graphene/PLA or graphene/ABS) has been proposed for the production of 3D-printed electrochemical biosensors [93]. In these devices, oxidoreductase enzymes, coupled with conductive electrodes, are able to transduce the biochemical interactions into a readable electronic signal [94].

Graphene-PLA composite filaments were used to print, by means of an FFF equipment, 3D working electrodes of an amperometric biosensor for glucose monitoring in blood plasma using glucose oxidase (GOx) and ferrocene-carboxylic acid as a mediator [95], with a simultaneous determination of uric acid and nitrite. In this case, the COOH groups exposed on the surface of the 3D-printed graphene-PLA were used to immobilize the GOx enzyme that was then cross-linked with

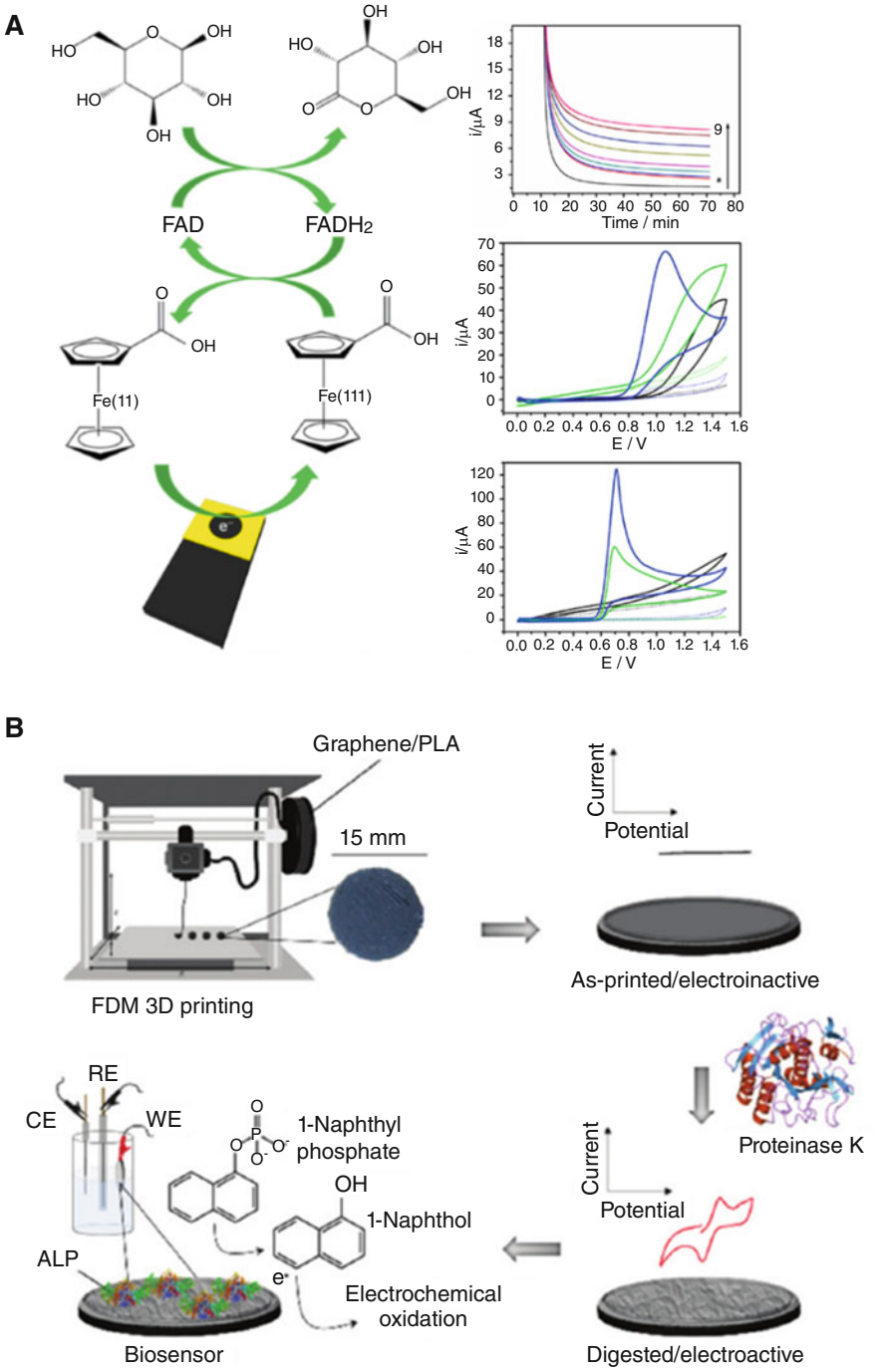

Fig. 7.3 (continued)

glutaraldehyde (Fig. 7.3a). The reported results showed a satisfactory detection of glucose at levels commonly found in blood samples: the chronoamperometric measurements gave a linear response for increasing concentrations of glucose with a limit of detection (LOD) of 15 μmol/L and LODs of 0.02 and 0.03 μmol/L for uric acid and nitrite, respectively.

3D-printed graphene-PLA electrodes were also proposed by Manzanares-Palenzuela et al. for the detection of 1-naphthol in contaminated wastewaters by cyclic voltammetry (CV) [96]. The device exploited the controlled degradation of PLA by using proteinase K, to activate the surface and achieve the controlled patterning of the 3D-printed surfaces to be used as working electrodes. Indeed, the as-printed surfaces are electrochemically irresponsive toward the ferro−/ferricyanide redox pair, whereas the proteinase K-mediated PLA hydrolysis exposes the embedded electroactive graphene and enhances the overall conductivity of the 3D-printed material and switches on the biosensors. On this activated surface, alkaline phosphatase was immobilized by adsorption to detect 1-naphthyl phosphate in solution (Fig. 7.3b). More recently, a new biosensor exploiting 3D-printed electrodes made of graphene-PLA was proposed by the same group [97].

This work described a 3D-printed electrochemical enzyme-based biosensor with a third-generation scheme of detection. The sensor did not need mediators because of the fast electron transfer between the redox enzyme and the electrode. The graphene-PLA 3D-printed electrodes were immersed in dimethylformamide or underwent the application of a constant potential to be electrochemically activated to enhance their conductivity. Two different configurations were evaluated for the detection of hydrogen peroxide: in one case, horseradish peroxidase (HRP) was directly immobilized onto the electrode surface, and in the second case, HRP was immobilized on the surface of the electrode previously decorated with gold nanoparticles. Both the configurations gave promising results from chronoamperometric measurements at different H_2O_2 concentrations with a LOD of 11.1 μM and 9.1 μM.

Fig. 7.3 (continued) (**a**) Scheme of the two steps of redox reactions exploited by the graphene-PLA composite biosensor to convert glucose into gluconolactone by using glucose oxidase and ferrocene-carboxylic acid. Insets: amperometric measurements of glucose (0–6.3 mmol/L) (top), cyclic voltammograms for 1.0 mmol/L uric acid (middle), and 1.0 mmol/L nitrite (bottom) recorded on the "as-printed" G-PLA electrode (black), after mechanical polishing (green) and solvent-treated after polishing (blue). Dashed lines correspond to the respective blanks (Reprinted from Ref. [95] with the permission from the WILEY-VCH Verlag). (**b**) Workflow of the fabrication steps of a 3D-printed graphene-PLA biosensor fabrication: the electrode is printed by FDM, and then the proteinase K-mediated PLA hydrolysis activates the surface, by exposing the electroactive graphene, because the as-printed electrodes are electrochemically irresponsive toward the ferro/ferricyanide redox pair. The immobilization of alkaline phosphatase allows the 1-naphthyl phosphate detection. (Reprinted from Ref. [96] with the permission from the Royal Society of Chemistry)

7.3.2 Flexible-Wearable Biosensors

A good part of the actually produced bioanalytical devices could envisage a great improvement if transformed into flexible-wearable electrochemical biosensor [98]. Above all, when applications in small metabolite monitoring are considered (e.g., glucose, lactose, or choline), medical devices using noninvasive approaches are requested. The possibility to make them wearable would represent a step forward in their development. To make this possible, the first requirement is flexibility that nowadays can be obtained by using smart textiles and stretchable electronics [99], often obtained by 3D printing with the subsequent addition of CNTs (carbon nanotubes), graphene, or metal nanoparticles [87].

The most suitable 3D printing technology to produce flexible electrodes and devices is DIW; this technique allows the design and patterning of highly precise enzyme-based POC (point-of-care) systems presenting uniform surface and few defects [100].

One example of DIW-printed flexible sensor was proposed by Dong and coworkers [101]. They produced a flexible amperometric lactate sensor based on a three-electrode configuration. A silver nanoparticle-based ink was extruded via DIW on a flexible polyethylene terephthalate (PET) substrate. A sulfonated fluoropolymer-copolymer, Nafion, was coated on the working electrode followed by the immobilization of the enzyme lactate oxidase. An oxidation peak at 0.25 V was revealed by CV (capacitance-voltage) measurements conducted at different lactate concentrations, and the amperometric biosensor gave a linear response as the lactate concentration increased from 0 to 15 mM.

Another example was given by Nesaei et al. that produced a flexible glucose biosensor [102]. A commercial carbon ink was modified with Prussian blue as electron transfer mediator, and in parallel, a GOx enzyme solution combined with tetraethoxysilane and hydroxypropyl cellulose to obtain a sol-gel printable ink was prepared. Both inks were 3D printed using DIW method (Fig. 7.4a). The chronoamperometric data revealed a linear oxidation current in the range of glucose concentration between 100 and 1000 mM; it was estimated a sensitivity of 17.5 nA/mM and a LOD of 6.9 mM.

Pu and colleagues used a rotating inkjet printing apparatus to obtain a micropatterning on a nonplanar surface to produce an implantable flexible enzyme-electrode sensor for continuous glucose monitoring [103]. A polyether ether ketone (PEEK) cylinder modified with silane agents was used as depositing substrate; a silver ink was used for the deposition of the counter and reference electrodes, while the working electrode was produced with a 3D multilayered nanostructure alternating the deposition of different inks containing gold nanoparticles, reduced graphene oxide (rGO), and Pt nanoparticles (PtNPs). The GOx enzyme was then printed onto the working electrode and covered by drop casting with Nafion to improve its biocompatibility and stability. The biosensor resulted capable to detect concentrations of glucose up to 570 mg/dL; this value results suitable for the detection in physiological conditions.

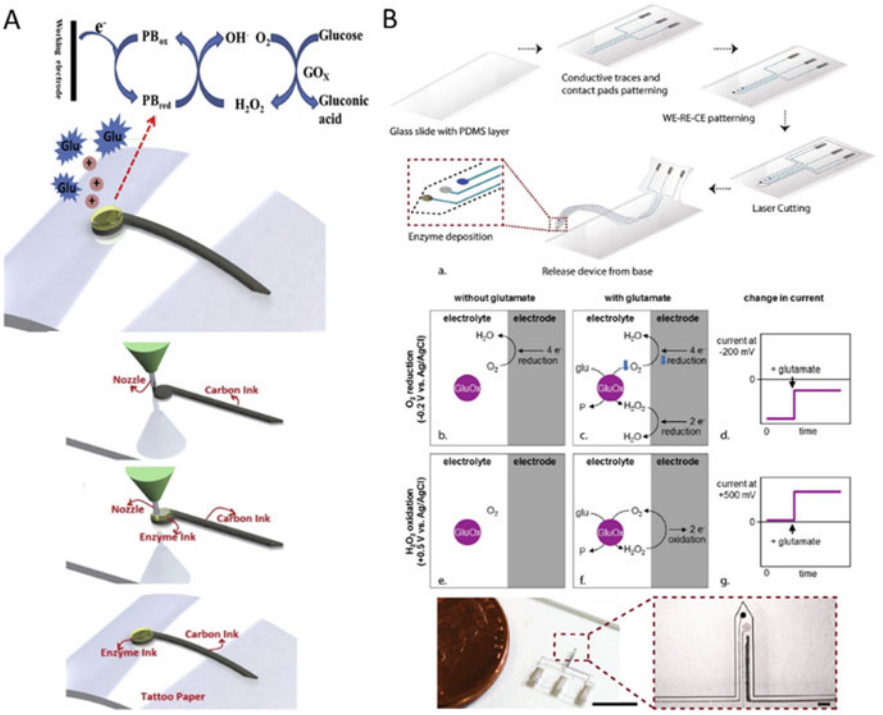

Fig. 7.4 (**a**) Workflow of the fabrication of the printed electrode by using a direct ink writing and an enzyme as printing materials on a flexible substrate (top); working principle of glucose sensing (Reprinted from Ref. [102] with the permission from the Elsevier B.V.) (**b**) Fabrication process of the PtNP-nanocomposite-based glutamate biosensor on a PDMS (polydimethylsiloxane) substrate (top); working principle of the biosensor (middle); picture of the micro-glutamate biosensor on PDMS substrate (scale bars: 5 mm and 200 μm). (Reprinted from Ref. [104] with the permission from the Elsevier B.V.)

An implantable amperometric biosensor for the evaluation of glutamate release from the spinal cord of a rat was also proposed in literature exploiting a similar approach [104].

A flexible silicone rubber (Ecoflex™) was mixed to conductive poly(3,4-ethylenedioxythiophene) polystyrene sulfonate (PEDOT:PSS), multiwalled carbon nanotubes, and platinum NPs for the production of the printable ink that was deposited by DIW on a flexible polymer substrate. Glutamate oxidase (GluOx) was used as sensing enzyme and immobilized on the electrodes with glutaraldehyde. This enzyme consumes O_2 to generate H_2O_2 that can be used for the amperometric evaluation of glutamate concentrations (Fig. 7.4b). It was observed that imposing a potential of 0.5 V vs. Ag/AgCl reference electrode, H_2O_2 is oxidized by the PtNPs, generating a current proportional to the concentration of glutamate, while at −0.2 V, the O_2 is reduced, generating a cathodic current that decreases when the enzyme consumes the oxygen in the presence of glutamate. Also, this system showed a

linear response in the range of 1–800 μM and a LOD of 0.5 μM when operated at 0.5 V and between 10 and 600 μM with a LOD of 0.2 μM when operated at −0.2 V.

The large number of printable biocompatible (nano)composites proposed for the production of scaffolds for tissue engineering and regenerative medicine [4] has opened the possibility to merge their properties with the versatility of the DIW technique leading to the production of flexible biosensors applied to the monitoring of cell culture metabolites. One example was given by Nolan et al. that produced a flexible biosensor array for the simultaneous monitoring of glucose, lactate, and glutamate from human astrocytes [105]. The active ink for the electrodes was formulated using PEDOT:PSS (poly(3,4-ethylenedioxythiophene) polystyrene sulfonate), silicone, activated carbon, and Pt microparticles. The immobilized enzymes glucose, lactate, and glutamate oxidases made the biosensor array selective toward the analytes of interest from astrocyte cultures at 37 °C. It was also demonstrated that the biosensor array can be printed onto different substrates such as cell culture plates, sheets of flexible laminates, and glass slides. Neuronal electrophysiology was also studied using a flexible biosensor exploiting a biocompatible graphene-based platform by Guo and coworkers [34]. The graphene ink was ink-jetted on a Kapton substrate where N27 neurons were cultured; the biocompatibility was assessed as cell survival after 72 h (85%).

7.3.3 Biocatalysis

In the previous sections, the different applications of enzyme-based biosensors and wearable electronics have been discussed. Enzyme-based devices demonstrated considerable capability in monitoring specific biomarkers in body fluids (e.g., sweat, saliva, tears, etc.) and in revealing environmental pollutants [106–109].

In the following paragraphs, biocatalytical devices will be discussed discerning pure enzymatical systems from bioreactors used for energy harvesting or for fine chemical synthesis.

7.3.3.1 Enzyme-Based Systems

Enzymes present catalytic activity and selectivity that can also be exploited for the development of analytical 3D-printed devices for biocatalysis. As it will be explained in the following paragraph, enzymes have been directly embedded in the printable material or immobilized on confined parts of the 3D-printed structures. Both strategies present some advantages and drawbacks.

Biosensors were built by 3D printing hydrogels embedding enzymes to obtain bioactive constructs with biomimetic capabilities [110]. PEGDA hydrogels were printed in the presence of alkaline phosphatase and thrombin as enzymes; AP catalyzes the formation and precipitation of calcium phosphate while thrombin

the formation of fibrin. The two enzymes co-immobilized into a bioinspired 3D object (mimicking bone tissue) led first to the calcification of the structure and subsequently to the covering of this last with a fibrin network, also able to entangle living cells. Despite the easiness and rapidity of the process, one of the main drawbacks of the direct incorporation of the enzymes in the printable materials are the preservation of the catalytic activity and the low long-term stability of the biomolecules.

Different studies were conducted, aiming to overcome these problems. One example is the work developed at the Karlsruhe Institute of Technology [111] where the stability problem was faced by testing different viscosity-enhancing additives. Polyxanthan, hectorite, and silica nanoparticles were tested to obtain stable PEGDA-based formulation embedding β-galactosidase (β-Gal). While polyxanthan and hectorite did not allow the formation of a mechanically stable 3D object, silica NPs allowed the production of good structures; nevertheless, the enzyme activity resulted to be only 10% compared to the free enzyme in solution, due to mass transfer limitations.

As an alternative, Wegner et al. [112] proposed a water-in-oil internal phase emulsion (HIPE)-encapsulating β-Gal as bioink for the 3D printing of scaffolds containing enzyme-loaded hydrogels. In this case, the new material showed a remarkable printability, with the possibility to print complex 3D geometries without the need of support structures. Also, the activity assays were performed on 3D-printed cylindrical-shaped constructs, evaluating the conversion of 2-nitrophenyl β-D-galactopyranoside (ONPG) to 2-nitrophenol (ONP) by spectrophotometry.

Original solutions were also reported trying to arrange low-cost and user-friendly apparatus, able to allow the 3D printing of enzyme-encapsulating materials for the realization of automated high-throughput screenings. As an example, Radtke et al. [113] implemented a common FFF printer for the encapsulation of active enzyme into hydrogels. As a proof of concept, PEGDA-based hydrogels, containing β-Gal, were again tested. In this case, a "mold-and-fill" procedure was followed in which a sacrificial ink was firstly used for the printing of hollow cylinders in a 48-wells plate, and then the space between the well rim and the printed cylinder was filled with liquid precursor of the PEGDA hydrogel containing β-Gal that was subsequently polymerized using a UV diode. The sacrificial structures could then be washed away at low temperature to obtain hollow structures with a height of 8 mm and a thickness of 1.6 mm. The catalytic activity of the enzyme was evaluated at different pH values by monitoring the formation of ONP from the substrate with a spectrophotometer.

A different flow bioreactor for the in vivo monitoring of glucose and lactate in the extracellular compartment of the rat brain was also printed by FFF by Su and colleagues [114]. An ABS flow reactor with two parallel reaction chambers, presenting a specific design aimed at enhancing the mixing effect and increasing the surface area, was built (Fig. 7.5a). The GOx enzyme was then immobilized onto the exposed surface in the inner part of the chambers, after its activation with glutaraldehyde; in the meantime, lactate oxidase was directly immobilized without the need for further modifications, thanks to the hydrophobic interactions with the styrene moieties of the ABS structure. The bioreactor was connected to a micro

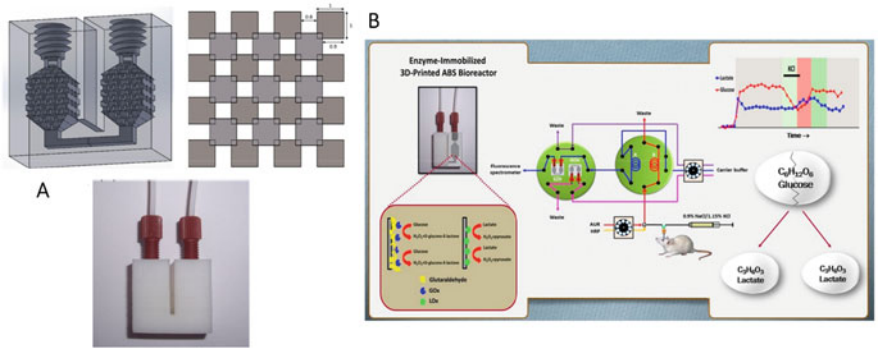

Fig. 7.5 (**a**) CAD drawings of the flow reactor, next to a layer of ordered cuboids in the reaction chamber. Below is a photograph of the printed reactor. (**b**) Scheme of the system for in vivo monitoring of the concentrations of rat brain's extracellular glucose and lactate. (Adapted from Ref. [114] Copyright 2016 American Chemical Society)

dialysis sampling probe and a spectrofluorometer. Aiming to evaluate the presence of glucose and lactate, the extracellular rat brain micro dialysate was mixed with HRP- and a H_2O_2-sensitive fluorogenic substrate. In this way, during the flux, HRP could recognize the H_2O_2 generated by the oxidation of glucose/lactate giving a fluorescence signal, thanks to its catalytic activity. The LOD of this detection system was assessed at 60 μM for glucose and 59 μM for lactate (Fig. 7.5b).

7.3.3.2 3D-Printed Bioreactors

Among the possible evolutions of 3D-printed materials embedding biocatalyst, the development of continuous-flow bioreactors for chemical synthesis or energy harvesting can surely be foreseen. The integration of enzymes that can provide high regio- and stereoselectivity, coupled with the enhanced 3D design, can become a point of innovation [115].

For this purpose, the deep understanding of the enzymes' behavior, including kinetics, stability, and immobilization strategies, is mandatory for the correct development of performing devices that can operate in continuous processes [116].

Starting with energy bio-applications, in most of the proposed case studies, the researchers proceed with the design and printing of the device with a subsequent functionalization and immobilization with the desired enzyme to obtain the required functionality. One example is the work proposed by Rewatkar and Goel. Here the researchers developed enzymatic biofuel cells (BFC) using a dual-extruder FFF 3D printer [117]. The BFC was designed as a Y-shaped microfluidic device in which the microchannels were produced with a simple PLA filament, while the electrodes were built from a conductive graphene/PLA composite (Fig. 7.5a). The graphene/PLA electrodes underwent an activation procedure in DMF [93] and were then modified by the immobilization of two enzymes: GOx was used on

the bioanode, while laccase was chosen for the biocathode. The performed tests revealed that the device presented an open circuit potential of 0.425 V and maximum peak power density of 4.15 $\mu W/cm^2$ at a current density of 13.36 $\mu A/cm^2$.

3D printing technology can also allow the design of reactors in which separated reactions can take place building up sequences of multistep biocatalytic reactions assuring the best reaction conditions for each step and avoiding unwanted side reactions or product inhibition.

Maier et al. produced 3D flow-reactor cartridges [118] by the FFF 3D printing of agarose-based enzyme-integrated hydrogels. As explained in the previous paragraphs, FFF requires relatively high processing temperatures to allow the deposition of the filament and the adhesion between layers; this can result problematic when enzymes must be embedded into the filament. For this reason, thermostable enzymes were chosen by Maier and coworkers, or other enzymes were modified by protein engineering methods to make them stable at the needed temperature. Firstly, agarose bioinks were prepared embedding an esterase (EstII) or an alcohol dehydrogenase (ADH) from the thermophilic microorganism *Alicyclobacillus acidocaldarius*; this ink was used to produce different structures. As proof of concept, the catalytic activity of the embedded enzymes was tested following two processes: in one case, the EstII activity was followed by immersing the loaded hydrogel in a solution containing 5(6)-carboxyfluorescein dihexyl ester as fluorogenic substrate and monitoring its de-esterification; in the meanwhile, ADH activity was assessed evaluating the catalyzed reduction of isobutyraldehyde to yield isobutanol.

The results showed that the catalytic activity of the two enzymes was not damaged by the deposition procedure that took place at 60 °C. As further step, a different enzyme, ketoisovalerate decarboxylase (KIVD) from the mesophilic organism *Lactococcus lactis*, was also modified by computational methods, random mutagenesis, and screening of a clone library to obtain thermostable variant suitable for the application in FFF printing. The selected mutation of the enzyme was embedded into the cartridge of a flow reactor aiming to get the ketoisovalerate conversion into isobutyraldehyde.

Exploiting the same concept, a 3D-printed enzyme-loaded agarose hydrogel was used to build part of a modular flow reactor for the production of a chemoenzymatic reaction cascade [119].

Phenacrylate decarboxylase from *Enterobacter* sp. was chosen as enzyme for the first reaction step of the reactor to catalyze the formation of 4-vinylphenol from *p*-coumaric acid; subsequently, a palladium-catalyzed Heck reaction promoted the coupling with iodobenzene for the formation of 4-hydroxystilbene showing the possibility to obtain cascade reactions. Despite the intriguing approach, the total yield of the reaction was relatively low (15%) (Fig. 7.6b).

A step further in the production of multi-reaction flow bioreactor is represented by the possibility of combining different enzymes in sequential reaction chambers, obtaining a real cascade bioreactor. This was reported by Franzreb group [120]. A reactor chamber (13×13 mm^2) was firstly built by PolyJet 3D printing using a polypropylene photopolymer and loaded with PEGDA-based hydrogels embedding three different enzymes that were printed with an extrusion-based machine (Fig.

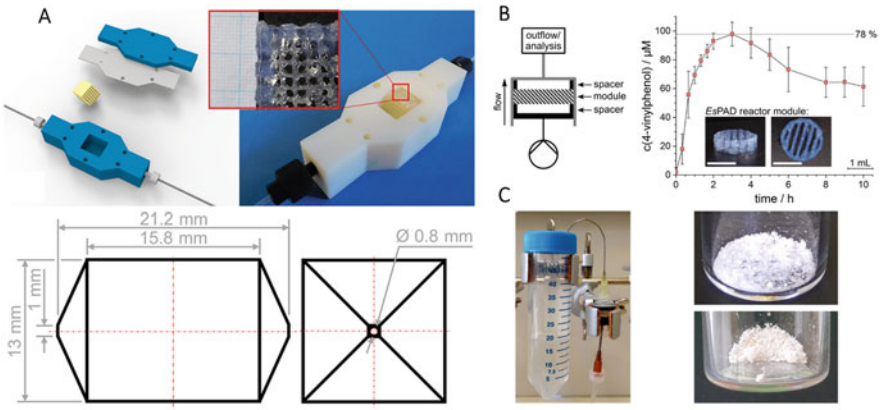

Fig. 7.6 (**a**) Reactor assembly, where the hydrogel structure is inserted in the reactor housing with connection to the fluidic system (Adapted from Ref. [120]). (**b**) Schematic setup of the flow reactor for flow experiments with one reactor module, next to a conversion of p-coumaric acid in a biocatalytic flow setup (Inset: 3D-printed reactor modules prior to assembly into the reactor). (**c**) Flow reactor setup of one out of four parallel reactors to produce 4-vinylphenol. The flow reactor next to the 50 mL collection tube is perfused with substrate solution by a syringe pump. On the right, the purified 4-vinylphenol (top) and, after subsequent Heck coupling, the purified 4-hydroxystilbene (bottom) are obtained as white crystals. (Adapted from Ref. [119] with the permission from the John Wiley and Sons)

7.6a). β-Galactosidase from *Aspergillus oryzae* (β-Gal), benzoylformate decarboxylase from *Pseudomonas putida* (BFD), and ADH from *Lactobacillus brevis* were chosen as enzymes. The first one allowed the selective hydrolysis of 2-nitrophenyl-β-D-galactopyranoside to 2-nitrophenol and galactose, while BFD and ADH were combined in a two-step reaction: firstly, BFD catalyzed the production of the intermediate (S)-2-hydroxy-1-phenyl-propanone by the carboligation of benzaldehyde and acetaldehyde; and then, the intermediate was further reduced to the product (1S,2S)-1-phenylpropane-1,2-diol by ADH. Finally, ADH was used for the enantioselective reduction of acetophenone to (R)-phenylethanol.

7.3.4 Precision Medicine

Patient-centered healthcare will represent the future of medicine, and for this reason, it has caught the attention of researcher operating in different biomedical sectors. Indeed, the possibility to provide customized treatments based on biological, physical, and medical differences of each individual is a challenging task that will greatly improve the success of medical treatments [121]; among the different possibilities, the patient-designed optimization of the dosage of a drug or medication has recently been considered. In this frame, 3D printing has been proposed for

the fabrication of tablets with customized dosage, multiple active pharmaceutical ingredients, and release profile [122].

7.3.4.1 Smart Tablets

Enteric, coated tablets were produced exploiting a dual-nozzle single step FFF 3D printing process [123]. The smart tablets were designed with a core-shell structure where the outer part, gastric-resistant, was produced with a methacrylic acid copolymer, presenting pH-dependent properties, while the inner structure was made of polyvinylpyrrolidone, using theophylline as a model drug. Budesonide and sodium diclofenac were also tested as drugs embedded in the core part, displaying a pH-sensitive drug release rate (Fig. 7.7a).

Fully customizable 3D-printed drug tablets were also proposed by Tan et al. [124]. Disc- and capsule-shaped tablets were produced using an extrusion-based 3D printer; the tables consisted of two surface-deteriorating matrices, one of those was incorporating the drug.

A biodegradable coating was deposited on the surface of the tablet excluding one side that was then directly exposed to the surrounding medium when in use. In this way, a precise control of the drug release profile over time could be achieved. The free surface, not loaded with the drug, was printed with different shaped cavities and used as a mold for the deposition of the drug-loaded matrix in order to provide a specifically designed release profile to the tablet. Paracetamol, phenylephrine hydrochloride, and diphenhydramine hydrochloride were tested as drugs demonstrating the possibility to achieve controlled release profiles. In the end, the customized and simultaneous release of two drugs, each with its own unique release profile, was also demonstrated (Fig. 7.7b).

Smart tablets have also been engineered aiming to achieve a better control over opioid abuse. Ong and coworkers fabricated tramadol tablets with alcohol-resistant and abuse-deterrent properties by direct powder extrusion 3D printing [125]. Hydroxypropyl cellulose was mixed with D-mannitol used as plasticizer, and tramadol hydrochloride was chosen as the active ingredient; polyethylene oxide was then added to the printable formulation as abuse-deterrent agent. The printed tablets demonstrated an abusive limitation potential of 13% when used with an intravenous route and of 70% with a nasal route, without alterations of the release profile in the presence of alcohol.

7.4 Conclusion

To summarize, in this chapter, the recent advances concerning 3D-printed devices with built-in (bio)chemical functionalities have been described, with particular emphasis on those exploitable to produce bioassay or enzyme-based objects for biotechnological applications. New potentials have been so demonstrated in several

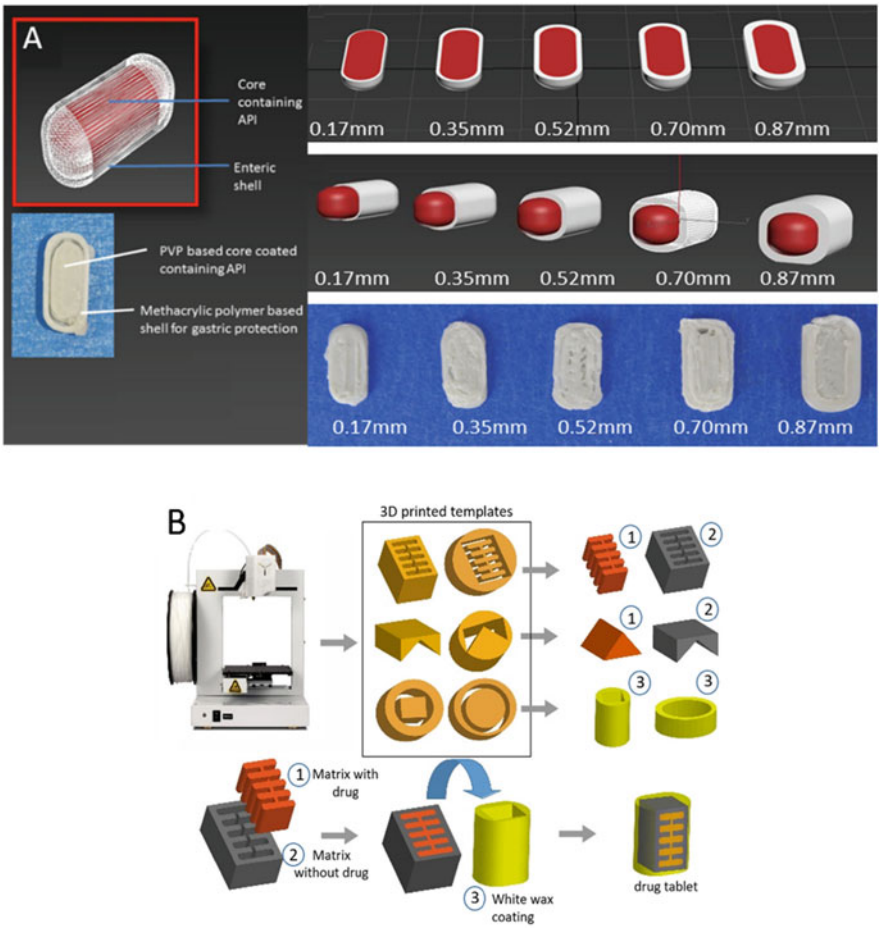

Fig. 7.7 (**a**) Schematic of shell-core designs with increasing shell thicknesses (0.17, 0.35, 0.52, 0.70, and 0.87 mm) and images of 30% completed shell-core designs with theophylline core and increasing shell thickness (Adapted from Ref. [123] with the permission from the Springer Nature). (**b**) Schematic of fabrication of the fully customizable drug tablet via 3D printing. (1) The matrix that contains the drug, (2) the matrix that does not contain the drug, and (3) the outer coating of white wax. Below is the process of fabricating the components via the molds and assembling the individual components into the drug tablet. (Reprinted from Ref. [124] with the permission from the Elsevier B.V.)

bio-application fields, such as biosensing or catalysis even in view of a broader implementation of precision medicine. The combination of functional materials with 3D printing generates different advantages, such as the rapid and versatile fabrication of items with fine-tuned materials, whose functionalities are designed taking in consideration the final use. This is mostly true in the development of bioanalytical LOC, which involve a careful blend of material and microfluidic design, trying to

improve recognition, immobilization, and stability of the biosensing elements. For instance, concerning immobilization, the entrapment of biological molecules in the whole polymeric matrix, or in selected parts of the object, can be obtained without any complex process, thanks to the layer-by-layer process.

In a nutshell, the structural and functional design of new devices is then expanded by the integration of both approaches, considering the benefits those techniques can offer when employed separately. Moreover, this strategy can be helpful also to improve the performance of routine methods in research laboratories, as reported for the well-known ELISA test. Nevertheless, even if different advantages can be listed out, some important challenges need to be resolved [126].

First of all, the physical and chemical properties of the materials should match with the printing mechanism. Therefore, a lot of work should be addressed to enhance the printability of materials containing the biomolecules responsible for the biochemical functionality of the object. Catalytical or biorecognition properties should be retained. At the same time, stability and processability should be preserved as well. Photopolymerization- or extrusion-based 3D printers, among the most exploited techniques, need harsh conditions such as high temperature or generate radical species, which are poorly compatible with the presence of antibodies, enzymes, nucleic acid probes, etc. Therefore, an effort to enhance the biocompatibility is awaited, in terms of stability (e.g., retained biological activity), or to cut mass transfer limitations off and keep the functions of the biomolecules. It must be noted that these aspects involve both the development of materials (e.g., novel photoinitiators) and biomolecule engineering (e.g., thermostability).

A secondary point is that on the market, there are specifically designed 3D printers for bio-application, the so-called bioprinter, but these are still costly and not intended for assembly production. In this view, any attempt such as the biomaker [113] reported above is welcomed.

At the same time, a further development can entail the combination of different 3D printing techniques in the same machine. Indeed, each technique shows its pros and cons. Then, the merging of various strategies may lead to multi-material objects with complexity tailored according to the final use. In this framework, well-established nanomaterials, already exploited in the conventional fabrication of bioanalytical devices, such as quantum dots or photonic crystals, have been only recently joined with 3D printing, giving rise to brand new technologies [127–129], or are still waiting for their integration with additive manufacturing. Finally, 3D printing offers the opportunity to get insights from the interaction between biology and material science, so that synergistic improvements are expected to foster fast and relevant unexplored advances in bio-applications.

References

1. N. Shahrubudin, T.C. Lee, R. Ramlan, An overview on 3D printing technology: Technological, materials, and applications. Procedia Manuf. **35**, 1286–1296 (2019). https://doi.org/10.1016/j.promfg.2019.06.089

2. Q. Yan, H. Dong, J. Su, J. Han, B. Song, Q. Wei, Y. Shi, A review of 3D printing technology for medical applications. Engineering **4**, 729–742 (2018). https://doi.org/10.1016/j.eng.2018.07.021
3. D.A. Kai, E.P. de Lima, M.W. Machado Cunico, S.E.G. da Costa, Additive manufacturing: A new paradigm for manufacturing. Proc. 2016 Ind. Syst. Eng. Res. Conf. ISERC **2016**, 452–457 (2016)
4. M. Hassan, K. Dave, R. Chandrawati, F. Dehghani, V.G. Gomes, 3D printing of biopolymer nanocomposites for tissue engineering: Nanomaterials, processing and structure-function relation. Eur. Polym. J. **121**, 109340 (2019). https://doi.org/10.1016/j.eurpolymj.2019.109340
5. X. Kuang, D.J. Roach, J. Wu, C.M. Hamel, Z. Ding, T. Wang, M.L. Dunn, H.J. Qi, Advances in 4D printing: Materials and applications. Adv. Funct. Mater. **29**, 1–23 (2019). https://doi.org/10.1002/adfm.201805290
6. C.A. Mandon, L.J. Blum, C.A. Marquette, Adding biomolecular recognition capability to 3D printed objects: 4D printing. Procedia Technol. **27**, 1–2 (2017). https://doi.org/10.1016/j.protcy.2017.04.001
7. S. Lantean, G. Barrera, C.F. Pirri, P. Tiberto, M. Sangermano, I. Roppolo, G. Rizza, 3D printing of magnetoresponsive polymeric materials with tunable mechanical and magnetic properties by digital light processing. Adv. Mater. Technol. **4**, 1–10 (2019). https://doi.org/10.1002/admt.201900505
8. S. Joshi, K.C.K. Rawat, V. Rajamohan, A.T. Mathew, K. Koziol, V. Kumar Thakur, A.S.S. Balan, 4D printing of materials for the future: Opportunities and challenges. Appl. Mater. Today **18**, 100490 (2020). https://doi.org/10.1016/j.apmt.2019.100490
9. M. Nadgorny, A. Ameli, Functional polymers and nanocomposites for 3D printing of smart structures and devices. ACS Appl. Mater. Interfaces **10**, 17489–17507 (2018). https://doi.org/10.1021/acsami.8b01786
10. H.N. Chan, M.J.A. Tan, H. Wu, Point-of-care testing: Applications of 3D printing. Lab Chip **17**, 2713–2739 (2017). https://doi.org/10.1039/c7lc00397h
11. C.K. Dixit, K. Kadimisetty, J. Rusling, 3D-printed miniaturized fluidic tools in chemistry and biology. TrAC – Trends Anal. Chem. **106**, 37–52 (2018). https://doi.org/10.1016/j.trac.2018.06.013
12. T. Han, S. Kundu, A. Nag, Y. Xu, 3D printed sensors for biomedical applications: A review. Sensors (Switzerland) **19** (2019). https://doi.org/10.3390/s19071706
13. J.F. Rusling, Developing microfluidic sensing devices using 3D printing. ACS Sensors **3**, 522–526 (2018). https://doi.org/10.1021/acssensors.8b00079
14. E. Dogan, A. Bhusal, B. Cecen, A.K. Miri, 3D printing metamaterials towards tissue engineering. Appl. Mater. Today **20** (2020). https://doi.org/10.1016/j.apmt.2020.100752
15. T. Genova, I. Roato, M. Carossa, C. Motta, D. Cavagnetto, F. Mussano, Advances on bone substitutes through 3d bioprinting. Int. J. Mol. Sci. **21**, 1–28 (2020). https://doi.org/10.3390/ijms21197012
16. J. He, B. Zhang, Z. Li, M. Mao, J. Li, K. Han, D. Li, High-resolution electrohydrodynamic bioprinting: A new biofabrication strategy for biomimetic micro/nanoscale architectures and living tissue constructs. Biofabrication **12** (2020). https://doi.org/10.1088/1758-5090/aba1fa
17. J. Li, C. Wu, P.K. Chu, M. Gelinsky, 3D printing of hydrogels: Rational design strategies and emerging biomedical applications. Mater. Sci. Eng. R. Rep. **140**, 100543 (2020). https://doi.org/10.1016/j.mser.2020.100543
18. C. Duty, C. Ajinjeru, V. Kishore, B. Compton, N. Hmeidat, X. Chen, P. Liu, A.A. Hassen, J. Lindahl, V. Kunc, What makes a material printable? A viscoelastic model for extrusion-based 3D printing of polymers. J. Manuf. Process. **35**, 526–537 (2018). https://doi.org/10.1016/j.jmapro.2018.08.008
19. S.A.M. Tofail, E.P. Koumoulos, A. Bandyopadhyay, S. Bose, L. O'Donoghue, C. Charitidis, Additive manufacturing: Scientific and technological challenges, market uptake and opportunities. Mater. Today **21**, 22–37 (2018). https://doi.org/10.1016/j.mattod.2017.07.001

20. S. Yuan, F. Shen, C.K. Chua, K. Zhou, Polymeric composites for powder-based additive manufacturing: Materials and applications. Prog. Polym. Sci. **91**, 141–168 (2019). https://doi.org/10.1016/j.progpolymsci.2018.11.001
21. X. Wang, M. Jiang, Z. Zhou, J. Gou, D. Hui, 3D printing of polymer matrix composites: A review and prospective. Compos. Part B Eng. **110**, 442–458 (2017). https://doi.org/10.1016/j.compositesb.2016.11.034
22. A. Bagheri, J. Jin, Photopolymerization in 3D printing. ACS Appl. Polym. Mater. **1**, 593–611 (2019). https://doi.org/10.1021/acsapm.8b00165
23. D. Popescu, A. Zapciu, C. Amza, F. Baciu, R. Marinescu, FDM process parameters influence over the mechanical properties of polymer specimens: A review. Polym. Test. **69**, 157–166 (2018). https://doi.org/10.1016/j.polymertesting.2018.05.020
24. M. Dzemko, B. Engelmann, J. Hartmann, J. Schmitt, Toward shifted production strategies through additive manufacturing: A technology and market review for changing value chains. Procedia CIRP **86**, 228–233 (2020). https://doi.org/10.1016/j.procir.2020.01.029
25. M. Harris, J. Potgieter, R. Archer, K.M. Arif, Effect of material and process specific factors on the strength of printed parts in fused filament fabrication: A review of recent developments. Materials (Basel) **12** (2019). https://doi.org/10.3390/ma12101664
26. F. Fenollosa, J.R. Gomà, I. Buj-Corral, A.T. Otero, J. Minguella-Canela, R. Uceda, A. Valls, M. Ayats, Foreseeing new multi-material FFF-additive manufacturing concepts meeting mimicking requirements with living tissues. Procedia Manuf. **41**, 1063–1070 (2019). https://doi.org/10.1016/j.promfg.2019.10.034
27. L.R. Lopes, A.F. Silva, O.S. Carneiro, Multi-material 3D printing: The relevance of materials affinity on the boundary interface performance. Addit. Manuf. **23**, 45–52 (2018). https://doi.org/10.1016/j.addma.2018.06.027
28. E. Cuan-Urquizo, E. Barocio, V. Tejada-Ortigoza, R.B. Pipes, C.A. Rodriguez, A. Roman-Flores, Characterization of the mechanical properties of FFF structures and materials: A review on the experimental, computational and theoretical approaches. Materials (Basel) **16** (2019). https://doi.org/10.3390/ma12060895
29. S.C. Daminabo, S. Goel, S.A. Grammatikos, H.Y. Nezhad, V.K. Thakur, Fused deposition modeling-based additive manufacturing (3D printing): Techniques for polymer material systems. Mater. Today Chem. **16**, 100248 (2020). https://doi.org/10.1016/j.mtchem.2020.100248
30. L. Li, Q. Lin, M. Tang, A.J.E. Duncan, C. Ke, Advanced polymer designs for direct-ink-write 3D printing. Chem. – A Eur. J. **25**, 10768–10781 (2019). https://doi.org/10.1002/chem.201900975
31. M.O. Aydogdu, B. Mutlu, M. Kurt, A.T. Inan, S.E. Kuruca, G. Erdemir, Y.M. Sahin, N. Ekren, F.N. Oktar, O. Gunduz, Developments of 3D polycaprolactone/beta-tricalcium phosphate/collagen scaffolds for hard tissue engineering. J. Aust. Ceram. Soc. **55**, 849–855 (2019). https://doi.org/10.1007/s41779-018-00299-y
32. Z. Ji, D. Jiang, X. Zhang, Y. Guo, X. Wang, Facile photo and thermal two-stage curing for high-performance 3D printing of poly(dimethylsiloxane). Macromol. Rapid Commun. **41**, 1–8 (2020). https://doi.org/10.1002/marc.202000064
33. M.A. Skylar-Scott, J. Mueller, C.W. Visser, J.A. Lewis, Voxelated soft matter via multimaterial multinozzle 3D printing. Nature **575**, 330–335 (2019). https://doi.org/10.1038/s41586-019-1736-8
34. Y. Guo, J. Xu, C. Yan, Y. Chen, X. Zhang, X. Jia, Y. Liu, X. Wang, F. Zhou, Direct ink writing of high performance architectured polyimides with low dimensional shrinkage. Adv. Eng. Mater. **21**, 1–8 (2019). https://doi.org/10.1002/adem.201801314
35. T. Mohan, A. Dobaj Štiglic, M. Beaumont, J. Konnerth, F. Gürer, D. Makuc, U. Maver, L. Gradišnik, J. Plavec, R. Kargl, K. Stana Kleinschek, Generic method for designing self-standing and dual porous 3D bioscaffolds from cellulosic nanomaterials for tissue engineering applications. ACS Appl. Bio Mater. **3**, 1197–1209 (2020). https://doi.org/10.1021/acsabm.9b01099

36. R. Karyappa, A. Ohno, M. Hashimoto, Immersion precipitation 3D printing (ip3DP). Mater. Horizons **6**, 1834–1844 (2019)
37. W. Sun, B. Starly, A.C. Daly, J.A. Burdick, J. Groll, G. Skeldon, W. Shu, Y. Sakai, M. Shinohara, M. Nishikawa, J. Jang, D.W. Cho, M. Nie, S. Takeuchi, S. Ostrovidov, A. Khademhosseini, R.D. Kamm, V. Mironov, L. Moroni, I.T. Ozbolat, The bioprinting roadmap. Biofabrication **12** (2020). https://doi.org/10.1088/1758-5090/ab5158
38. I. Matai, G. Kaur, A. Seyedsalehi, A. McClinton, C.T. Laurencin, Progress in 3D bioprinting technology for tissue/organ regenerative engineering. Biomaterials **226**, 119536 (2020). https://doi.org/10.1016/j.biomaterials.2019.119536
39. I.T. Ozbolat, M. Hospodiuk, Current advances and future perspectives in extrusion-based bioprinting. Biomaterials **76**, 321–343 (2016). https://doi.org/10.1016/j.biomaterials.2015.10.076
40. T. Bhattacharjee, S.M. Zehnder, K.G. Rowe, S. Jain, R.M. Nixon, W.G. Sawyer, T.E. Angelini, Writing in the granular gel medium. Sci. Adv. **1**, 4–10 (2015). https://doi.org/10.1126/sciadv.1500655
41. W. Liu, Z. Zhong, N. Hu, Y. Zhou, L. Maggio, A.K. Miri, A. Fragasso, X. Jin, A. Khademhosseini, Y.S. Zhang, Coaxial extrusion bioprinting of 3D microfibrous constructs with cell-favorable gelatin methacryloyl microenvironments. Biofabrication **10** (2018). https://doi.org/10.1088/1758-5090/aa9d44
42. J.H. Galarraga, M.Y. Kwon, J.A. Burdick, 3D bioprinting via an in situ crosslinking technique towards engineering cartilage tissue. Sci. Rep. **9**, 1–12 (2019). https://doi.org/10.1038/s41598-019-56117-3
43. M. Mobaraki, M. Ghaffari, A. Yazdanpanah, Y. Luo, D.K. Mills, Bioinks and bioprinting: A focused review. Bioprinting **18**, e00080 (2020). https://doi.org/10.1016/j.bprint.2020.e00080
44. R.R. Jose, M.J. Rodriguez, T.A. Dixon, F. Omenetto, D.L. Kaplan, Evolution of bioinks and additive manufacturing technologies for 3D bioprinting. ACS Biomater Sci. Eng. **2**, 1662–1678 (2016). https://doi.org/10.1021/acsbiomaterials.6b00088
45. A.K. Miri, E. Mostafavi, D. Khorsandi, S.K. Hu, M. Malpica, A. Khademhosseini, Bioprinters for organs-on-chips. Biofabrication **11** (2019). https://doi.org/10.1088/1758-5090/ab2798
46. S.C. Ligon, R. Liska, J. Stampfl, M. Gurr, R. Mülhaupt, Polymers for 3D printing and customized additive manufacturing. Chem. Rev. **117**, 10212–10290 (2017). https://doi.org/10.1021/acs.chemrev.7b00074
47. L.Y. Zhou, J. Fu, Y. He, A review of 3D printing technologies for soft polymer materials. Adv. Funct. Mater. **2000187**, 1–38 (2020). https://doi.org/10.1002/adfm.202000187
48. Hull, C.W., Spence, S.T., Albert, D.J., Smalley, D.R., Harlow, R.A. Steinbaugh, P., Tarnoff, H.L., Nguyen, H.D., Lewis, C.W., Vorgitch, T.J., 1991. *Methods and Apparatus for Production of Three-Dimensional Objects by Stereolithography*
49. J.R. Tumbleston, D. Shirvanyants, N. Ermoshkin, R. Janusziewicz, A.R. Johnson, D. Kelly, K. Chen, R. Pinschmidt, J.P. Rolland, A. Ermoshkin, E.T. Samulski, J.M. DeSimone, Continuous liquid interface production of 3D objects. Science (80-.) **347**, 1349–1352 (2015). https://doi.org/10.1126/science.aaa2397
50. M. Shusteff, A.E.M. Browar, B.E. Kelly, J. Henriksson, T.H. Weisgraber, R.M. Panas, N.X. Fang, C.M. Spadaccini, One-step volumetric additive manufacturing of complex polymer structures. Sci. Adv. **3** (2017). https://doi.org/10.1126/sciadv.aao5496
51. J. Zhang, P. Xiao, 3D printing of photopolymers. Polym. Chem. **9**, 1530–1540 (2018). https://doi.org/10.1039/c8py00157j
52. L.K. Fai, C.C. Kai, T.C. Hock, Microblasting characteristics of jewellery models built using stereolithography apparatus (SLA). Int. J. Adv. Manuf. Technol. **14**, 450–458 (1998)
53. M. Revilla-León, M. Sadeghpour, M. Özcan, An update on applications of 3D printing technologies used for processing polymers used in implant dentistry. Odontology **108**, 331–338 (2020). https://doi.org/10.1007/s10266-019-00441-7
54. B. Heidt, R. Rogosic, S. Bonni, J. Passariello-Jansen, D. Dimech, J.W. Lowdon, R. Arreguin-Campos, E. Steen Redeker, K. Eersels, H. Diliën, B. van Grinsven, T.J. Cleij, The liberalization of microfluidics: Form 2 benchtop 3D printing as an affordable alternative

to established manufacturing methods. Phys. Status Solid. Appl. Mater. Sci. **1900935**, 1–7 (2020). https://doi.org/10.1002/pssa.201900935
55. C. Liu, N. Huang, F. Xu, J. Tong, Z. Chen, X. Gui, Y. Fu, C. Lao, 3D printing technologies for flexible tactile sensors toward wearable electronics and electronic skin. Polymers (Basel) **10**, 1–31 (2018). https://doi.org/10.3390/polym10060629
56. M. Zarek, M. Layani, I. Cooperstein, E. Sachyani, D. Cohn, S. Magdassi, 3D printing of shape memory polymers for flexible electronic devices. Adv. Mater. **28**, 4449–4454 (2016)
57. K.S. Lim, J.H. Galarraga, X. Cui, G.C.J. Lindberg, J.A. Burdick, T.B.F. Woodfield, Fundamentals and applications of photo-cross-linking in bioprinting. Chem. Rev. (2020). https://doi.org/10.1021/acs.chemrev.9b00812
58. H. Quan, T. Zhang, H. Xu, S. Luo, J. Nie, X. Zhu, Photo-curing 3D printing technique and its challenges. Bioact. Mater. **5**, 110–115 (2020). https://doi.org/10.1016/j.bioactmat.2019.12.003
59. X. Zhou, Y. Hou, J. Lin, A review on the processing accuracy of two-photon polymerization. AIP Adv. **5** (2015). https://doi.org/10.1063/1.4916886
60. J.T. Fourkas, Fundamentals of two-photon fabrication, in *Three-Dimensional Microfabrication Using Two-Photon Polymerization*, (William Andrew Publishing, 2020), pp. 57–76
61. C.K. Ober, Materials systems for 2-photon lithography, in *Three-Dimensional Microfabrication Using Two-Photon Polymerization2*, (William Andrew Publishing, 2020), pp. 143–174
62. J. Song, C. Michas, C.S. Chen, A.E. White, M.W. Grinstaff, From simple to architecturally complex hydrogel scaffolds for cell and tissue engineering applications: Opportunities presented by two-photon polymerization. Adv. Healthc. Mater. **9**, 1–13 (2020). https://doi.org/10.1002/adhm.201901217
63. C.W. Ha, P. Prabhakaran, K.S. Lee, Versatile applications of three-dimensional objects fabricated by two-photon-initiated polymerization. MRS Commun. **9**, 53–66 (2019). https://doi.org/10.1557/mrc.2018.218
64. J. Li, P. Fejes, D. Lorenser, B.C. Quirk, P.B. Noble, R.W. Kirk, A. Orth, F.M. Wood, B.C. Gibson, D.D. Sampson, R.A. McLaughlin, Two-photon polymerisation 3D printed freeform micro-optics for optical coherence tomography fibre probes. Sci. Rep. **8**, 1–9 (2018). https://doi.org/10.1038/s41598-018-32407-0
65. S. Rodríguez, Redefining microfabrication of high-precision optics. PhotonicsViews **17**, 36–39 (2020). https://doi.org/10.1002/phvs.202000003
66. A.T. Gaynor, N.A. Meisel, C.B. Williams, J.K. Guest, Multiple-material topology optimization of compliant mechanisms created via Poly jet three-dimensional printing. J. Manuf. Sci. Eng. Trans. ASME **136**, 1–10 (2014). https://doi.org/10.1115/1.4028439
67. S. Tibbits, *4D Printing: Multi-Material Shape Change* (2014), pp. 421–433. https://doi.org/10.1142/9789811201493_0027
68. N.P. Macdonald, J.M. Cabot, P. Smejkal, R.M. Guijt, B. Paull, M.C. Breadmore, Comparing microfluidic performance of three-dimensional (3D) printing platforms. Anal. Chem. **89**, 3858–3866 (2017a). https://doi.org/10.1021/acs.analchem.7b00136
69. R.D. Sochol, E. Sweet, C.C. Glick, S. Venkatesh, A. Avetisyan, K.F. Ekman, A. Raulinaitis, A. Tsai, A. Wienkers, K. Korner, K. Hanson, A. Long, B.J. Hightower, G. Slatton, D.C. Burnett, T.L. Massey, K. Iwai, L.P. Lee, K.S.J. Pister, L. Lin, 3D printed microfluidic circuitry via multijet-based additive manufacturing. Lab Chip **16**, 668–678 (2016). https://doi.org/10.1039/c5lc01389e
70. M. Pohanka, Three-dimensional printing in analytical chemistry: Principles and applications. Anal. Lett. **49**, 2865–2882 (2016). https://doi.org/10.1080/00032719.2016.1166370
71. M. Belka, L. Konieczna, M. Okońska, M. Pyszka, S. Ulenberg, T. Bączek, Application of 3D-printed scabbard-like sorbent for sample preparation in bioanalysis expanded to 96-wellplate high-throughput format. Anal. Chim. Acta **1081**, 1–5 (2019). https://doi.org/10.1016/j.aca.2019.05.078
72. L.P.C. Gomez, A. Spangenberg, X.A. Ton, Y. Fuchs, F. Bokeloh, J.P. Malval, B. Tse Sum Bui, D. Thuau, C. Ayela, K. Haupt, O. Soppera, Rapid prototyping of chemical microsensors based on molecularly imprinted polymers synthesized by two-photon stereolithography. Adv. Mater. **28**, 5931–5937 (2016). https://doi.org/10.1002/adma.201600218

73. G. De Middeleer, P. Dubruel, S. De Saeger, Molecularly imprinted polymers immobilized on 3D printed scaffolds as novel solid phase extraction sorbent for metergoline. Anal. Chim. Acta **986**, 57–70 (2017). https://doi.org/10.1016/j.aca.2017.07.059
74. M. Gou, X. Qu, W. Zhu, M. Xiang, J. Yang, K. Zhang, Y. Wei, S. Chen, Bio-inspired detoxification using 3d-printed hydrogel nanocomposites. Nat. Commun. **5**, 1–9 (2014). https://doi.org/10.1038/ncomms4774
75. N.P. Macdonald, S.A. Currivan, L. Tedone, B. Paull, Direct production of microstructured surfaces for planar chromatography using 3D printing. Anal. Chem. **89**, 2457–2463 (2017b). https://doi.org/10.1021/acs.analchem.6b04546
76. E.K. Parker, A.V. Nielsen, M.J. Beauchamp, H.M. Almughamsi, J.B. Nielsen, M. Sonker, H. Gong, G.P. Nordin, A.T. Woolley, 3D printed microfluidic devices with immunoaffinity monoliths for extraction of preterm birth biomarkers. Anal. Bioanal. Chem. **411**, 5405–5413 (2019). https://doi.org/10.1007/s00216-018-1440-9
77. M. Belka, S. Ulenberg, T. Bączek, Fused deposition modeling enables the low-cost fabrication of porous, customized-shape sorbents for small-molecule extraction. Anal. Chem. **89**, 4373–4376 (2017). https://doi.org/10.1021/acs.analchem.6b04390
78. G. Palmara, F. Frascella, I. Roppolo, A. Chiappone, A. Chiadò, Functional 3D printing: Approaches and bioapplications. Biosens. Bioelectron. **175**, 112849 (2021). https://doi.org/10.1016/j.bios.2020.112849
79. R. Calmo, A. Chiadò, S. Fiorilli, C. Ricciardi, Advanced ELISA-like biosensing based on ultralarge-pore silica microbeads. ACS Appl. Bio Mater. **3**, 5787–5795 (2020). https://doi.org/10.1021/acsabm.0c00533
80. D. Sticker, R. Geczy, U.O. Häfeli, J.P. Kutter, Thiol-Ene based polymers as versatile materials for microfluidic devices for life sciences applications. ACS Appl. Mater. Interfaces **12**, 10080–10095 (2020). https://doi.org/10.1021/acsami.9b22050
81. C.A. Mandon, L.J. Blum, C.A. Marquette, Adding biomolecular recognition capability to 3D printed objects. Anal. Chem. **88**, 10767–10772 (2016). https://doi.org/10.1021/acs.analchem.6b03426
82. S. Stassi, E. Fantino, R. Calmo, A. Chiappone, M. Gillono, D. Scaiola, C.F. Pirri, C. Ricciardi, A. Chiadò, I. Roppolo, Polymeric 3D printed functional microcantilevers for biosensing applications. ACS Appl. Mater. Interfaces **9**, 19193–19201 (2017). https://doi.org/10.1021/acsami.7b04030
83. C. Credi, G. Griffini, M. Levi, S. Turri, Biotinylated photopolymers for 3D-printed unibody lab-on-a-chip optical platforms. Small **14**, 1–8 (2018). https://doi.org/10.1002/smll.201702831
84. C. Aronsson, M. Jury, S. Naeimipour, F.R. Boroojeni, J. Christoffersson, P. Lifwergren, C.F. Mandenius, R. Selegård, D. Aili, Dynamic peptide-folding mediated biofunctionalization and modulation of hydrogels for 4D bioprinting. Biofabrication **12** (2020). https://doi.org/10.1088/1758-5090/ab9490
85. Y. Ukita, Y. Utsumi, Y. Takamura, Direct digital manufacturing of a mini-centrifuge-driven centrifugal microfluidic device and demonstration of a smartphone-based colorimetric enzyme-linked immunosorbent assay. Anal. Methods **8**, 256–262 (2015). https://doi.org/10.1039/c5ay01969a
86. A. Chiadò, G. Palmara, A. Chiappone, C. Tanzanu, C.F. Pirri, I. Roppolo, F. Frascella, A modular 3D printed lab-on-a-chip for early cancer detection. Lab Chip **20**, 665–674 (2020). https://doi.org/10.1039/c9lc01108k
87. H. Singh, M. Shimojima, S. Fukushi, A. Le Van, M. Sugamata, M. Yang, Increased sensitivity of 3D-well enzymelinked immunosorbent assay (ELISA) for infectious disease detection using 3Dprinting fabrication technology. Biomed. Mater. Eng. **26**, S45–S53 (2015a). https://doi.org/10.3233/BME-151288
88. H. Singh, M. Shimojima, T. Shiratori, L. Van An, M. Sugamata, M. Yang, Application of 3D printing technology in increasing the diagnostic performance of enzyme-linked immunosorbent assay (ELISA) for infectious diseases. Sensors (Switzerland) **15**, 16503–16515 (2015b). https://doi.org/10.3390/s150716503

89. T. Distler, A.R. Boccaccini, 3D printing of electrically conductive hydrogels for tissue engineering and biosensors – A review. Acta Biomater. **101**, 1–13 (2020). https://doi.org/10.1016/j.actbio.2019.08.044
90. D. Lin, S. Jin, F. Zhang, C. Wang, Y. Wang, C. Zhou, G.J. Cheng, 3D stereolithography printing of graphene oxide reinforced complex architectures. Nanotechnology **26** (2015). https://doi.org/10.1088/0957-4484/26/43/434003
91. F. Frascella, G. González, P. Bosch, A. Angelini, A. Chiappone, M. Sangermano, C.F. Pirri, I. Roppolo, Three-dimensional printed photoluminescent polymeric waveguides. ACS Appl. Mater. Interfaces **10**, 39319–39326 (2018). https://doi.org/10.1021/acsami.8b16036
92. M. Gillono, I. Roppolo, F. Frascella, L. Scaltrito, C.F. Pirri, A. Chiappone, CO2 permeability control in 3D printed light responsive structures. Appl. Mater. Today **18**, 100470 (2020). https://doi.org/10.1016/j.apmt.2019.100470
93. C.L. Manzanares Palenzuela, M. Pumera, (Bio)analytical chemistry enabled by 3D printing: Sensors and biosensors. TrAC – Trends Anal. Chem. **103**, 110–118 (2018). https://doi.org/10.1016/j.trac.2018.03.016
94. J. Muñoz, M. Pumera, 3D-printed biosensors for electrochemical and optical applications. TrAC – Trends Anal. Chem. **128**, 115933 (2020). https://doi.org/10.1016/j.trac.2020.115933
95. R.M. Cardoso, P.R.L. Silva, A.P. Lima, D.P. Rocha, T.C. Oliveira, T.M. do Prado, E.L. Fava, O. Fatibello-Filho, E.M. Richter, R.A.A. Muñoz, 3D-printed graphene/polylactic acid electrode for bioanalysis: Biosensing of glucose and simultaneous determination of uric acid and nitrite in biological fluids. Sensors Actuators B Chem. **307**, 127621 (2020). https://doi.org/10.1016/j.snb.2019.127621
96. C.L. Manzanares-Palenzuela, S. Hermanova, Z. Sofer, M. Pumera, Proteinase-sculptured 3D-printed graphene/polylactic acid electrodes as potential biosensing platforms: Towards enzymatic modeling of 3D-printed structures. Nanoscale **11**, 12124–12131 (2019). https://doi.org/10.1039/c9nr02754h
97. A.M. López Marzo, C.C. Mayorga-Martinez, M. Pumera, 3D-printed graphene direct electron transfer enzyme biosensors. Biosens. Bioelectron. **151** (2020). https://doi.org/10.1016/j.bios.2019.111980
98. H. Lin, Y. Zhao, S. Lin, B. Wang, C. Yeung, X. Cheng, Z. Wang, T. Cai, W. Yu, K. King, J. Tan, K. Salahi, H. Hojaiji, S. Emaminejad, A rapid and low-cost fabrication and integration scheme to render 3D microfluidic architectures for wearable biofluid sampling, manipulation, and sensing. Lab Chip **19**, 2844–2853 (2019). https://doi.org/10.1039/c9lc00418a
99. H.C. Koydemir, A. Ozcan, Wearable, epidermal, and implantable sensors for biomedical applications. Annu. Rev. Anal. Chem. **11**, 1–20 (2018)
100. J.A. Lewis, Direct ink writing of 3D functional materials. Adv. Funct. Mater. **16**, 2193–2204 (2006). https://doi.org/10.1002/adfm.200600434
101. Y. Dong, X. Min, W.S. Kim, A 3-D-printed integrated PCB-based electrochemical sensor system. IEEE Sensors J. **18**, 2959–2966 (2018). https://doi.org/10.1109/JSEN.2018.2801459
102. S. Nesaei, Y. Song, Y. Wang, X. Ruan, D. Du, A. Gozen, Y. Lin, Micro additive manufacturing of glucose biosensors: A feasibility study. Anal. Chim. Acta **1043**, 142–149 (2018). https://doi.org/10.1016/j.aca.2018.09.012
103. Z. Pu, J. Tu, R. Han, X. Zhang, J. Wu, C. Fang, H. Wu, X. Zhang, H. Yu, D. Li, A flexible enzyme-electrode sensor with cylindrical working electrode modified with a 3D nanostructure for implantable continuous glucose monitoring. Lab Chip **18**, 3570–3577 (2018). https://doi.org/10.1039/c8lc00908b
104. T.N.H. Nguyen, J.K. Nolan, H. Park, S. Lam, M. Fattah, J.C. Page, H.E. Joe, M.B.G. Jun, H. Lee, S.J. Kim, R. Shi, H. Lee, Facile fabrication of flexible glutamate biosensor using direct writing of platinum nanoparticle-based nanocomposite ink. Biosens. Bioelectron. **131**, 257–266 (2019). https://doi.org/10.1016/j.bios.2019.01.051
105. J.K. Nolan, T.N.H. Nguyen, K.V.H. Le, L.E. DeLong, H. Lee, Simple fabrication of flexible biosensor arrays using direct writing for multianalyte measurement from human astrocytes. SLAS Technol. **25**, 33–46 (2019). https://doi.org/10.1177/2472630319888442

106. J. Kim, I. Jeerapan, J.R. Sempionatto, A. Barfidokht, R.K. Mishra, A.S. Campbell, L.J. Hubble, J. Wang, Wearable bioelectronics: Enzyme-based body-worn electronic devices. Acc. Chem. Res. **51**, 2820–2828 (2018). https://doi.org/10.1021/acs.accounts.8b00451
107. J. Kim, G. Valdés-Ramírez, A.J. Bandodkar, W. Jia, A.G. Martinez, R. Julian, P. Mercier, J. Wang, Non-invasive mouthguard biosensor for continuous salivary monitoring of metabolites. Analyst **139**, 1632–1636 (2014). https://doi.org/10.1039/c3an02359a
108. A. Martín, J. Kim, J.F. Kurniawan, J.R. Sempionatto, J.R. Moreto, G. Tang, A.S. Campbell, A. Shin, M.Y. Lee, X. Liu, J. Wang, Epidermal microfluidic electrochemical detection system: Enhanced sweat sampling and metabolite detection. ACS Sensors **2**, 1860–1868 (2017). https://doi.org/10.1021/acssensors.7b00729
109. R. Zou, S. Shan, L. Huang, Z. Chen, T. Lawson, M. Lin, L. Yan, Y. Liu, High-performance intraocular biosensors from chitosan-functionalized nitrogen-containing graphene for the detection of glucose. ACS Biomater Sci. Eng. **6**, 673–679 (2020). https://doi.org/10.1021/acsbiomaterials.9b01149
110. C.D. Devillard, C.A. Mandon, S.A. Lambert, L.J. Blum, C.A. Marquette, Bioinspired multi-activities 4D printing objects: A new approach toward complex tissue engineering. Biotechnol. J. **13**, 1–8 (2018). https://doi.org/10.1002/biot.201800098
111. B. Schmieg, J. Döbber, F. Kirschhöfer, M. Pohl, M. Franzreb, Advantages of hydrogel-based 3D-printed enzyme reactors and their limitations for biocatalysis. Front. Bioeng. Biotechnol. **6**, 1–12 (2019). https://doi.org/10.3389/fbioe.2018.00211
112. L. Wenger, C.P. Radtke, J. Göpper, M. Wörner, J. Hubbuch, 3D-printable and enzymatically active composite materials based on hydrogel-filled high internal phase emulsions. Front. Bioeng. Biotechnol. **8**, 1–17 (2020). https://doi.org/10.3389/fbioe.2020.00713
113. C.P. Radtke, N. Hillebrandt, J. Hubbuch, The biomaker: An entry-level bioprinting device for biotechnological applications. J. Chem. Technol. Biotechnol. **93**, 792–799 (2018a). https://doi.org/10.1002/jctb.5429
114. C.K. Su, S.C. Yen, T.W. Li, Y.C. Sun, Enzyme-immobilized 3D-printed reactors for online monitoring of rat brain extracellular glucose and lactate. Anal. Chem. **88**, 6265–6273 (2016). https://doi.org/10.1021/acs.analchem.6b00272
115. L. Tamborini, P. Fernandes, F. Paradisi, F. Molinari, Flow bioreactors as complementary tools for biocatalytic process intensification. Trends Biotechnol. **36**, 73–88 (2018). https://doi.org/10.1016/j.tibtech.2017.09.005
116. C. Zhao, N. Zhang, H. Zheng, Q. Zhu, M. Utsumi, Y. Yang, Effective and long-term continuous bio-hydrogen production by optimizing fixed-bed material in the bioreactor. Process Biochem. **83**, 55–63 (2019). https://doi.org/10.1016/j.procbio.2019.04.021
117. C.P. Radtke, N. Hillebrandt, J. Hubbuch, The biomaker: An entry-level bioprinting device for biotechnological applications. J. Chem. Technol. Biotechnol. **93**, 792–799 (2018b). https://doi.org/10.1002/jctb.5429
118. M. Maier, C.P. Radtke, J. Hubbuch, C.M. Niemeyer, K.S. Rabe, On-demand production of flow-reactor cartridges by 3D printing of thermostable enzymes. Angew. Chem. Int. Ed. **57**, 5539–5543 (2018). https://doi.org/10.1002/anie.201711072
119. M. Peng, E. Mittmann, L. Wenger, J. Hubbuch, M.K.M. Engqvist, C.M. Niemeyer, K.S. Rabe, 3D-printed phenacrylate decarboxylase flow reactors for the chemoenzymatic synthesis of 4-Hydroxystilbene. Chem. – A Eur. J. **25**, 15998–16001 (2019). https://doi.org/10.1002/chem.201904206
120. B. Schmieg, A. Schimek, M. Franzreb, Development and performance of a 3D-printable poly(ethylene glycol) diacrylate hydrogel suitable for enzyme entrapment and long-term biocatalytic applications. Eng. Life Sci. **18**, 659–667 (2018). https://doi.org/10.1002/elsc.201800030
121. A. Awad, S.J. Trenfield, S. Gaisford, A.W. Basit, 3D printed medicines: A new branch of digital healthcare. Int. J. Pharm. **548**, 586–596 (2018). https://doi.org/10.1016/j.ijpharm.2018.07.024
122. M.A. Alhnan, T.C. Okwuosa, M. Sadia, K.W. Wan, W. Ahmed, B. Arafat, Emergence of 3D printed dosage forms: Opportunities and challenges. Pharm. Res. **33**, 1817–1832 (2016). https://doi.org/10.1007/s11095-016-1933-1

123. T.C. Okwuosa, B.C. Pereira, B. Arafat, M. Cieszynska, A. Isreb, M.A. Alhnan, Fabricating a shell-core delayed release tablet using dual FDM 3D printing for patient-centred therapy. Pharm. Res. **34**, 427–437 (2017). https://doi.org/10.1007/s11095-016-2073-3
124. Y.J.N. Tan, W.P. Yong, J.S. Kochhar, J. Khanolkar, X. Yao, Y. Sun, C.K. Ao, S. Soh, On-demand fully customizable drug tablets via 3D printing technology for personalized medicine. J. Control. Release **322**, 42–52 (2020). https://doi.org/10.1016/j.jconrel.2020.02.046
125. J.J. Ong, A. Awad, A. Martorana, S. Gaisford, E. Stoyanov, A.W. Basit, A. Goyanes, 3D printed opioid medicines with alcohol-resistant and abuse-deterrent properties. Int. J. Pharm. **579**, 119169 (2020). https://doi.org/10.1016/j.ijpharm.2020.119169
126. G. Palmara, A. Chiadò, R. Calmo, C. Ricciardi, Succinic anhydride functionalized microcantilevers for protein immobilization and quantification. Anal. Bioanal. Chem. **408**, 7917–7926 (2016). https://doi.org/10.1007/s00216-016-9920-2
127. J. Bae, S. Lee, J. Ahn, J.H. Kim, M. Wajahat, W.S. Chang, S.Y. Yoon, J.T. Kim, S.K. Seol, J. Pyo, 3D-printed quantum dot nanopixels. ACS Nano **14**, 10993–11001 (2020). https://doi.org/10.1021/acsnano.0c04075
128. C.D. Brubaker, T.M. Frecker, J.R. McBride, K.R. Reid, G.K. Jennings, S.J. Rosenthal, D.E. Adams, Incorporation of fluorescent quantum dots for 3D printing and additive manufacturing applications. J. Mater. Chem. C **6**, 7584–7593 (2018). https://doi.org/10.1039/c8tc02024h
129. Y. Liu, H. Wang, J. Ho, R.C. Ng, R.J.H. Ng, V.H. Hall-Chen, E.H.H. Koay, Z. Dong, H. Liu, C.W. Qiu, J.R. Greer, J.K.W. Yang, Structural color three-dimensional printing by shrinking photonic crystals. Nat. Commun. **10** (2019). https://doi.org/10.1038/s41467-019-12360-w